JOURNAL OF GEOPHYSICAL RESEARCH, VOL. 106, NO. C12, PAGES 31,489-31,509, DECEMBER 15, 2001

Moored sediment trap measurements of carbon export in the Subantarctic and Polar Frontal Zones of the Southern Ocean, south of Australia

T. W. Trull and S. G. Bray

Antarctic Cooperative Research Centre, Hobart, Tasmania, Australia

S. J. Manganini, S. Honjo, and R. François

Woods Hole Oceanographic Institution, Woods Hole, Massachusetts. USA

Abstract. Sediment trap moorings were deployed from September 21, 1997 through February 21, 1998 at three locations south of Australia along 140°E: at ~47°S in the central Subantarctic Zone (SAZ) with traps at 1060, 2050, and 3850 m depth, at ~51°S in the Subantarctic Front with one trap at 3080 m, and at ~54°S in the Polar Frontal Zone (PFZ) with traps at 830 and 1580 m. Particle fluxes were high at all the sites (18-32 g m^{-2} yr^{-1} total mass and 0.5-1.4 g organic carbon m^{-2} yr^{-1} at ~1000 m, assuming minimal flux outside the sampled summer period). These values are similar to other Southern Ocean results and to the median estimated for the global ocean by Lampitt and Antia [1997], and emphasize that the Southern Ocean exports considerable carbon to the deep sea despite its "high-nutrient, low chlorophyll" characteristics. The SAZ site was dominated by carbonate (>50% of total mass) and the PFZ site by biogenic silica (>50% of total mass). Both sites exhibited high export in spring and late summer, with an intervening low flux period in December. For the 153 day collection period, particulate organic carbon export was somewhat higher in all the traps in the SAZ (range 0.57-0.84 gC m^{-2}) than in the PFZ (range 0.31-0.53), with an intermediate value observed at the SAF (0.60). The fraction of surface organic carbon export (estimated from seasonal nutrient depletion, Lourey and Trull [2001]) reaching 1000 m was indistinguishable in the SAZ and PFZ, despite different algal communities.

1. Introduction

1.1. Importance of Biological Carbon Export

Particles sinking from the surface to the deep sea redistribute the ocean's content of dissolved carbon. This process plays a major role in controlling atmospheric carbon dioxide levels, and variations in the sinking particle flux are a likely cause of atmospheric CO_2 changes on intra-annual to century, millennial, and glacial-inter-glacial timescales [*Lee et al.*, 1998; *Sarmiento and LeQuere*, 1996; *Sarmiento et al.*, 1988; *Shaffer*, 1993]. The Southern Ocean is a particularly important region in this control because the global overturning thermohaline circulation brings carbon dioxide-rich deep waters to its surface [*Caldeira and Duffy*, 2000; *Matear and Hirst*, 1999; *Sarmiento and Bender*, 1994]. Biological uptake of this carbon reduces the extent of its transfer to the atmosphere but is far from complete, with much of the Southern Ocean containing high levels of nutrients in surface waters and low abundances of phytoplankton. Changes in the magnitude of Southern Ocean biological production [*Kumar et al.*, 1995], the extent of communication between its surface and deep waters [*Francois et al.*, 1997], and the limitation of air-sea gas exchange by sea ice [*Stephens and Keeling*, 2000] have been suggested as possible origins of lowered atmospheric pCO_2 during the Last Glacial Maximum. There has also been considerable speculation that productivity changes may have been driven by the availability of iron [*Lefevre and Watson*, 1999; *Martin et al.*, 1990], which has recently been demonstrated to enhance phytoplankton production in the modern Southern Ocean in open ocean iron fertilization experiments [*Boyd et al.*, 2000; *Smetacek*, 2001], although enhanced particle export was not observed during these short experiments.

Despite the recognized importance of biological carbon export in the Southern Ocean, there has been very little study of modern Southern Ocean sinking particle fluxes to the deep sea. A recent global review identified only three studies, all in the Atlantic sector [*Lampitt and Antia*, 1997]. Two of these were in embayment systems (Bransfield Strait and the Weddell Sea), with just one in circumpolar waters, near the Polar Front. This sparsity of results, and the extremely low fluxes recorded by the Weddell Sea site, for which the possibility of a technical problem had been raised [*Jacques*, 1991], led Lampitt and Antia to suggest that Antarctic fluxes differ significantly in character from other regions of the global ocean. Since then several major programs have reported moored particle flux results (as summarized in Table 1). These programs have had a major focus on the shallow Antarctic margins but have also included some open Southern Ocean studies, particularly in the vicinity of the Antarctic

Paper number 2000JC000308.
0148-0227/01/2000JC000308$09.00

Table 1. Southern Ocean Sediment Trap Fluxes[a]

Region	Latitude	Longitude	Start Date	End Date	Duration, days	Bottom Depth, m	Trap Depth bsl, m	Total Mass Flux g m^{-2} yr^{-1}	POC mass flux g m^{-2} yr^{-1}	Source
Deep Ocean, Ice Free										
Pacific (AESOPS 1)	53.0°S	174.7°W	Nov. 28, 1996	Jan. 18, 1998	416	5441	1981	12	1.0	*Honjo et al.* [2000]
Pacific (AESOPS 2)	56.9°S	170.2°W	Nov. 28, 1996	Jan. 18, 1998	416	4924	982	34	1.7	*Honjo et al.* [2000]
Pacific (AESOPS 3)	60.3°S	170.1°W	Nov. 28, 1996	Jan. 01, 1998	399	3957	1003	57	2.3	*Honjo et al.* [2000]
Pacific (AESOPS 4)	63.2°S	169.9°W	Nov. 28, 1996	Jan. 01, 1998	399	2885	1031	81	2.2	*Honjo et al.* [2000]
Pacific (AESOPS 5)	66.2°S	169.7°W	Nov. 28, 1996	Jan. 01, 1998	399	3015	937	28	1.9	*Honjo et al.* [2000]
SW Pacific, N Chatham Rise	42.7°S	178.6°E	Sept. 14, 1996	May 15, 1997	243	1500	1000	161	7.5	*Nodder and Northcote* [2001]
SW Pacific, S Chatham Rise	44.6°S	178.6°E	June 09, 1996	May 15, 1997	340	1500	1000	11	1.8	*Nodder and Northcote* [2001]
Atlantic, Bouvet Island	54.3°S	3.4°W	Dec. 28, 1990	Dec. 31, 1991	368	2734	450	84	2.7	*Fischer et al.* [2000]
Atlantic, Bouvet Island	54.3°S	3.4°W	May 15, 1992	Dec. 01, 1992	200	2965	456	20	0.9	*Fischer et al.* [2000]
Atlantic	50.1°S	5.9°W	Jan. 15, 1987	Mar. 12, 1988	421	3750	700	38	2.9	*Wefer and Fischer* [1991]
Atlantic	50.1°S	5.9°W	Nov. 10, 1989	Dec. 23, 1990	408	3785	614	54	3.4	*Fischer et al.* [2000]
Indian, Kerguelen Islands	50.7°S	68.4°E	April. 09, 1993	Jan. 14, 1995	640	1755	200	11	0.7	*Miquel et al.* [1998]
Indian	46.8°S	142.1°E	Sept. 21, 1997	Feb. 21, 1998	153	4540	1060	18	1.4	this study
Indian	46.8°S	142.1°E	Sept. 21, 1997	Feb. 21, 1998	153	4540	2050	23	1.3	this study
Indian	46.8°S	142.1°E	Sept. 21, 1997	Feb. 21, 1998	153	4540	3850	20	1.0	this study
Indian	51.0°S	141.7°E	Sept. 21, 1997	Feb. 21, 1998	153	3780	3080	32	0.8	this study
Indian	53.8°S	141.8°E	Sept. 21, 1997	Feb. 21, 1998	153	2280	830	27	0.8	this study
Indian	46.8°S	142.1°E	Sept. 21, 1997	Feb. 21, 1998	153	2280	1580	22	0.5	this study
Shallow Ocean and Ice Zones										
Ross Sea (AESOPS 6)	73.6°S	176.9°E	Nov. 28, 1996	Jan. 18, 1998	416	565	460	16	1.9	*Collier et al.* [2000]
Ross Sea (AESOPS 7)	76.5°S	177.9°W	Nov. 28, 1996	Jan. 18, 1998	416	566	465	62	11	*Collier et al.* [2000]
Ross Ice Shelf	78.0°S	177.0°W	Jan. 28, 1995	Jan. 21, 1996	358	602	423	6.2	0.6	*Accornero et al.* [1999]
Ross Sea	76.5°S	167.5°E	Jan. 13, 1990	Feb. 07, 1992	755	769	250	71	5.0	*Dunbar et al.* [1998]
Ross Sea	76.5°S	167.5°E	Jan. 13, 1990	Feb. 07, 1992	755	769	719	99	4.8	*Dunbar et al.* [1998]
Ross Sea	76.5°S	175.0°W	Jan. 17, 1990	Feb. 09, 1992	753	569	250	57	7.0	*Dunbar et al.* [1998]
Ross Sea	76.5°S	175.0°W	Jan. 17, 1990	Feb. 09, 1992	753	569	519	39	4.1	*Dunbar et al.* [1998]
Ross Sea	72.5°S	172.5°W	Jan. 22, 1990	Feb. 22, 1992	761	543	250	29	3.9	*Dunbar et al.* [1998]
Ross Sea	72.5°S	172.5°W	Jan. 22, 1990	Feb. 22, 1992	761	543	493	32	1.0	*Dunbar et al.* [1998]
Ross Sea	74.0°S	175.1°E	Dec. 15, 1994	Jan. 12, 1996	393	588	200	3.9	0.4	*Langone et al.* [2000]
Weddell Gyre	63.2°S	42.7°W	June 12, 1905	June 14, 1905	721	3793	2966	1.4	0.1	*Pudsey and King* [1997]
Weddell Gyre	62.1°S	40.6°W	June 12, 1905	June 14, 1905	722	3280	2453	3.4	0.2	*Pudsey and King* [1997]
Weddell Sea, Maud Rise	64.9°S	2.5°W	Jan. 20, 1987	Nov. 20, 1987	304	5000	4456	7.9	0.2	*Wefer and Fischer* [1991]
Weddell Sea, Maud Rise	64.9°S	2.6°W	Jan. 16, 1988	Feb. 04, 1989	384	5053	360	34	2.3	*Wefer and Fischer* [1991]
Weddell Sea, Maud Rise	64.9°S	2.6°W	Mar. 03, 1989	Feb. 26, 1990	360	5044	352	2.4	0.2	*Wefer and Fischer* [1991]
Weddell Sea	62.4°S	34.8°W	Jan. 25, 1985	Mar. 19, 1986	418	3880	863	0.2	0.01	*Fischer et al.* [1988]
Bransfield Strait	62.3°S	57.5°W	Dec. 31, 1983	Nov. 25, 1984	330	1952	494	120	2.2	*Wefer et al.* [1988]
Bransfield Strait	62.3°S	57.5°W	Dec. 01, 1983	Nov. 25, 1984	360	1952	1588	109	2.4	*Wefer et al.* [1988]
Bransfield Strait	62.2°S	57.5°W	Dec. 04, 1984	Nov. 13, 1985	343	1650	693	13	0.3	*Wefer and Fischer* [1991]
Bransfield Strait	62.2°S	57.5°W	Nov. 26, 1985	May 07, 1986	162	1992	687	82	0.5	*Wefer and Fischer* [1991]
Global compilation median								22	1.0	*Lampitt and Antia* [1997]

[a] Values shown are as reported. Conditions of collection vary strongly, and no normalization for collection duration or variations in protocols (e.g. preservative used, size fraction analyzed, treatment of "swimmers," etc.) has been made. See original references for details. POC, particulate organic carbon; bsl, below sea level.

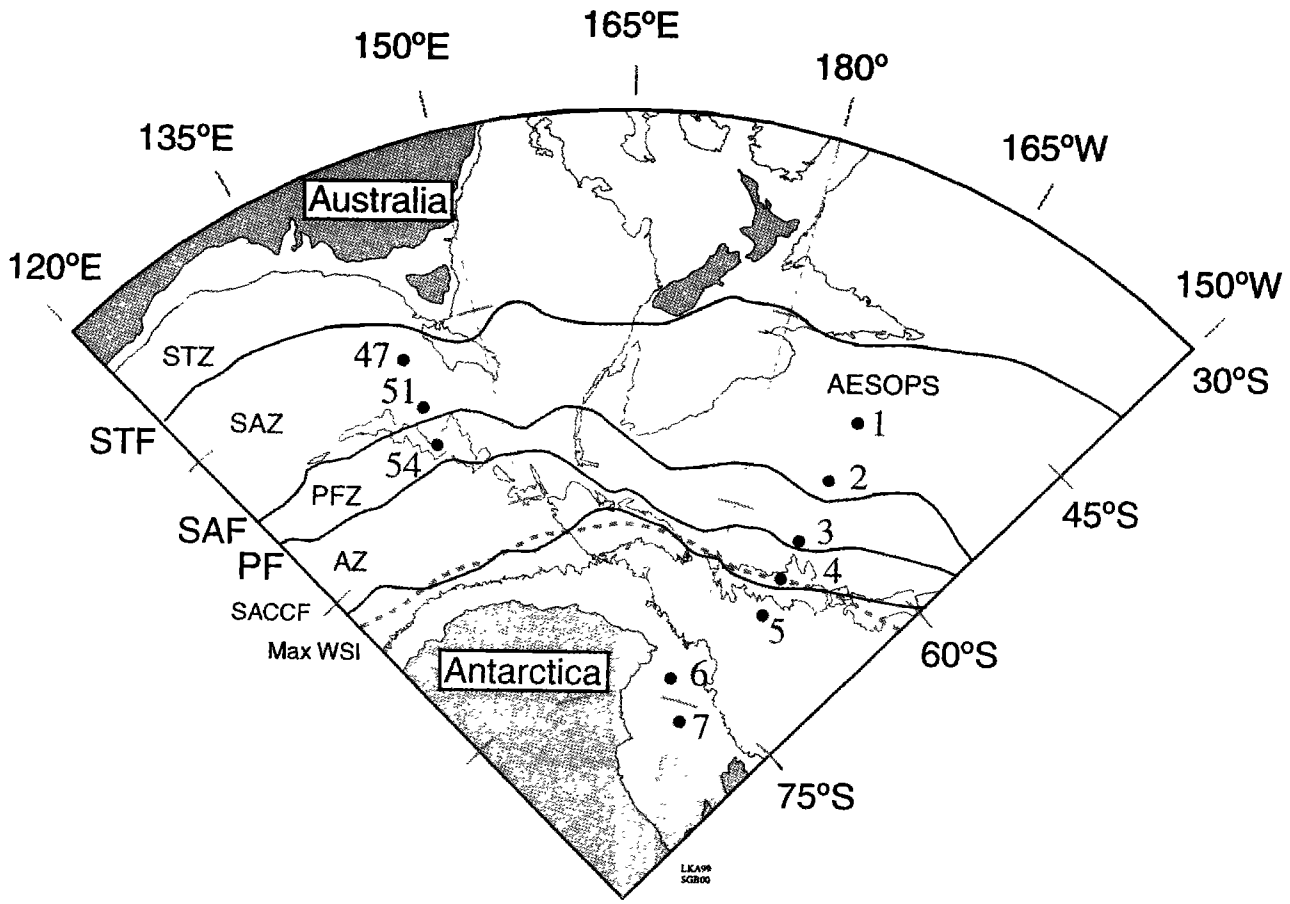

Figure 1. Map of the SAZ Project sediment trap mooring locations in relation to the oceanographic fronts and zones of the Southern Ocean [*Orsi et al.*, 1995]. Also shown for comparison are the locations of the Antarctic Environmental Southern Ocean Process Study (AESOPS) program particle flux traps [*Collier et al.*, 2000; *Honjo et al.*, 2000], and the 3000 m bathymetric contour. All the SAZ Project moorings were well north of the maximum extent of winter sea ice (Max WSI). As illustrated in Figure 9 and discussed in the text, the Subantarctic Front (SAF) was always north of the SAZ Project 51°S mooring during the 1997-1998 deployment year. PF, Polar Front; STF, Subtropical Front; SACCF, southern Antarctic Circumpolar Current Front; SAZ, Subantarctic Zone; PFZ, Polar Frontal Zone; AZ, Antarctic Zone; and STZ, Subtropical Zone.

Polar Front. Virtually all the recent studies have found relatively high annual fluxes (Table 1), similar to or higher than the median estimated from a compilation of results for the global open ocean [*Lampitt and Antia*, 1997].

1.2. Study Focus

At the inception of our project, no study had examined particle fluxes in the Subantarctic Zone (SAZ) of the Southern Ocean, despite the fact that the SAZ represents a large portion of the total area of the Southern Ocean (Figure 1), serves as a strong sink for atmospheric CO_2 (~1 Gt C yr^{-1} [*Metzl et al.*, 1999]), and is central to hypotheses linking particle fluxes and climate change [*Francois et al.*, 1997; *Kumar et al.*, 1995; *Sigman et al.*, 1999]. The SAZ serves as an interface between the cold nutrient-rich waters to its south and the nutrient-depleted subtropical gyres to its north. SAZ upper layers are marked by a thick layer of relatively homogenous Subantarctic Mode Water (SAMW), which overlies Antarctic Intermediate Water (AAIW, Figure 2). Both water masses are subducted northward beneath the subtropical gyres. Thus particles leaving the surface in these regions contribute to carbon redistribution via both the fraction that reaches the deep sea by settling and the fraction that is remineralized within SAMW or AAIW and subsequently subducted. The SAZ exhibits surface water carbon dioxide partial pressures well below atmospheric equilibrium, but PFZ waters are closer to atmospheric equilibrium in this sector [*Metzl et al.*, 1999; *Popp et al.*, 1999]. The relative physical and biological contributions to these carbon dioxide partial pressure variations are unclear, but it is important to determine them because physical and biological carbon dioxide transfers are expected to show different responses to climate change [*Matear et al.*, 1999; *Sarmiento and LeQuere*, 1996].

For these reasons we focused on the SAZ and, for comparative purposes, on the PFZ to its south. We measured particle fluxes using moored sinking particle traps at three sites in the SAZ, in the PFZ, and beneath the Subantarctic Front (SAF), which separates them (Figure 1). The Antarctic Environmental Southern Ocean Process Study (AESOPS) program also included a mooring in the SAZ, another at the SAF [*Honjo et al.*, 2000], and a pair of moorings north and

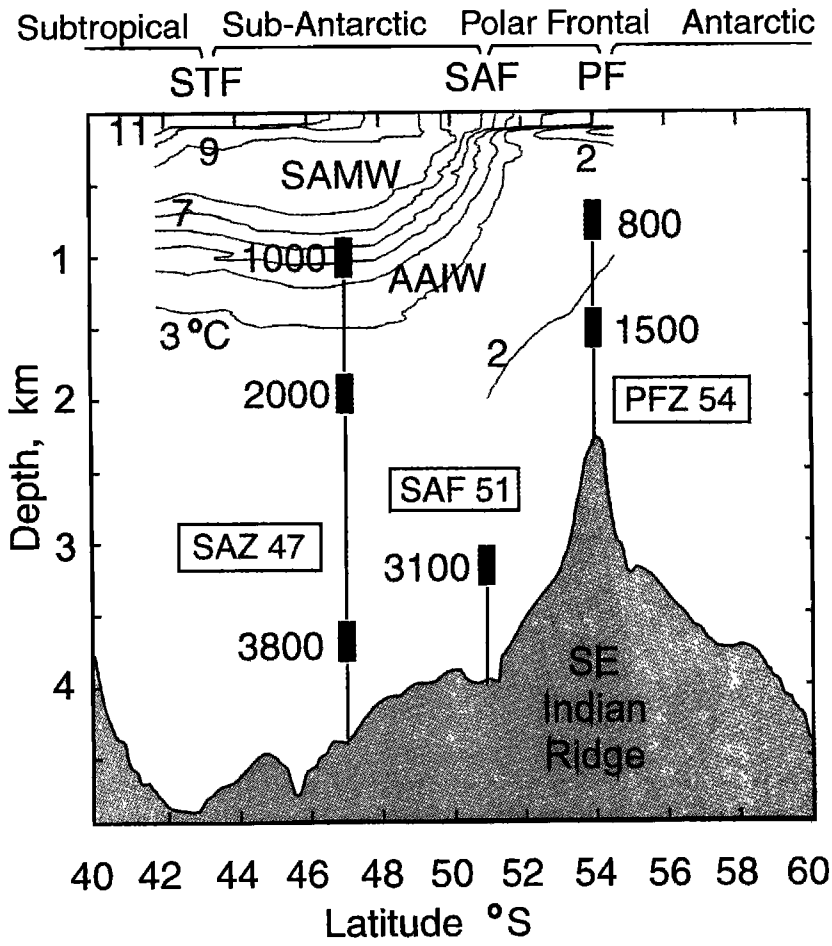

Figure 2. Cross section of the mooring locations in comparison to regional sea floor bathymetry and a late austral summer temperature section obtained in March 1998 at the time of mooring recovery. The mooring designations, SAZ 47, SAF 51, and PFZ 54 are used throughout the text, tables, and figures. SAMW, Subantarctic Mode Water; and AAIW, Antarctic Intermediate Water. Front and zone locations as they occurred during the 1997-1998 deployment year are marked at the top. Note the presence of the sub surface temperature minimum layer, marked by the 2°C isotherm at the PFZ 54 site.

south of the Sub-Tropical Front on the Chatham Rise east of New Zealand also sampled SAZ waters [*Nodder and Northcote*, 2001]. Brief comparisons to these results are provided in Table 1 and in more detail in section 3. Further description of regional oceanographic characteristics is provided in the section 4.

The choice of sites also allows the comparison of two quite different phytoplankton production regimes. SAZ waters in this region are dominated by nanophytoplankton and picophytoplankton, including carbonate-precipitating coccolithophores, other prymnesiophytes, cyanobacteria, and autotrophic flagellates, with lower abundances of diatoms [*Kopczynska et al.*, this issue; *Odate and Fukuchi*, 1995]. Biomass is often relatively homogeneously distributed throughout the mixed layer and moderately abundant [*Clementson et al.*, 1998; *Griffiths et al.*, 1999; *Popp et al.*, 1999]. In contrast, PFZ waters in this region contain more abundant and larger diatoms, as well as flagellates and coccolithophores, but few cyanobacteria [*Kopczynska et al.*, this issue; *Odate and Fukuchi*, 1995; *Popp et al.*, 1999; *Wright et al.*, 1996]. In the PFZ in this region a subsurface chlorophyll maximum layer within or beneath the seasonal pycnocline often occurs, particularly in summer, probably in response to iron and silicate colimitation within the mixed layer [*Parslow et al.*, this issue; *Popp et al.*, 1999]. The general characteristic of greater prevalence of large diatoms in the PFZ than in the SAZ, particularly during spring periods of enhanced production, has been documented in other sectors [*Bathmann et al.*, 1997; *Detmar and Bathmann*, 1997; *Smetacek et al.*, 1997; *van Leeuwe et al.*, 1998]. However, prymnesiophytes and autotrophic nanoflagellates and picoflagellates remain important and sometimes dominant components of PFZ phytoplankton biomass, both in terms of cell numbers and cell carbon budgets [*Buma et al.*, 1990; *Kopczynska et al.*, 1998; *Mengesha et al.*, 1998].

Given their strong differences in typical algal size classes, water column distributions, and absence or presence of diatoms, the SAZ and PFZ represent likely endmembers in the spectrum of ecosystem structures that produce low and high export, respectively, for a given level of production [*Boyd and Newton*, 1999; *Michaels and Silver*, 1988; *Smetacek*, 1985] and, to a lesser degree, in the extent of phytoplanktonic carbonate production, which tends to counter organic matter production in the control of surface carbon dioxide levels [*Holligan and Robertson*, 1996]. In addition, the SAZ mooring site provides some capability to assess the extent to

which elevated biomass accumulations along the front [*Bidigare et al.*, 1986; *Comiso et al.*, 1993; *Laubscher et al.*, 1993] lead to enhanced export.

2. Methods

The SAZ Project, organized by the Antarctic Cooperative Research Centre (CRC) with major contributions from the Commonwealth Scientific and Industrial Research Organisation (CSIRO) Division of Marine Research and Woods Hole Oceanographic Institution, has a continuing program of moored sediment trap studies in the SAZ and PFZ southwest of Tasmania along 140°E longitude. The first deployment, the subject of this paper, obtained samples weekly through the austral summer from September 1997 to February 1998 at three locations as shown in Figure 2: on the abyssal plane in the central SAZ (47°S, traps at ~1000, 2000, and 3800 m depth), beneath the SAF (51°S, trap at 3100 m), and on a local bathymetric high of the Southeast Indian Ridge in the PFZ (54°S, traps at 800 and 1500 m). Table 2 provides exact depths for the traps and additional information on the deployment sites. Cup rotation intervals are given in Table 3. Full details of the mooring designs, site geography, sample processing, archiving, and analytical methods are available in a technical report [*Bray et al.*, 2000].

All traps were large funnels with a baffle at the top (0.5 m^2 surface area) and a narrow opening at the bottom through which the particles fall into individual cups (McLane, Inc. Parflux 21 cup). Each trap was paired with an Aanderaa current meter and temperature sensor. The 250 mL sample cups were filled with unfiltered deep seawater from the region (collected at 1200 m depth, 49°17' S, 153°58' E), which was treated with 5 g L^{-1} sodium chloride to increase solution density, 1 g L^{-1} sodium tetraborate as a pH buffer, and 3 g L^{-1} mercuric chloride as a biocide. All the traps discussed here provided complete collection series (Table 3), without any instrumental failures. Measured currents were generally <10 cm s^{-1}, with occasional short excursions to higher velocities (Table 2), and tilt angles were very small (2° or less and quite constant [*Bray et al.*, 2000]). On the basis of global comparisons these mild conditions suggest that neither overcollection nor undercollection is likely to have occurred [*Honjo*, 1996; *Yu et al.*, 2001]. However, there are aspects of the measured fluxes that do raise the possibility of trapping efficiency variations, in particular, variations in total mass and ^{230}Th contents (as discussed further below).

The recovered cup solutions were allowed to settle, and aliquots of supernatant were drawn off with a syringe for dissolved nutrient, salinity, and pH measurements. The remaining sample slurries were then sieved through 1mm screen (no attempt to remove "swimmers" was made for the analyzed <1 mm fraction reported here). The <1 mm fraction was then split into 10 fractions using a rotating splitter (McLane, Inc.). Three of these tenths were filtered onto Nuclepore filters (0.45 μm pore size), removed from the filter as a wet cake of material, dried at 60°C, and ground in an agate mortar. This material was used to determine dry mass flux and all the other parameters reported here (except ^{230}Th, which was measured on a separate 1/10 split of the <1 mm fraction). Some cups contained very few particles, too little (<1 mg) to profitably sieve, split, and filter. These cups showed no evidence of initial solution loss (as determined by salinity and pH measurements [*Bray et al.*, 2000]) and therefore appear to represent truly low fluxes. They are listed in Table 3 as zero fluxes to emphasize that no flux was measured. No "blank" corrections were applied to any of the measured dry masses.

Particulate inorganic carbon (PIC) was determined by closed system acidification with phosphoric acid and coulometry. Particulate total carbon (PC) and nitrogen content (PN) were determined by unacidified combustion using a CHN analyzer. Particulate organic carbon (POC) was calculated from PC by subtraction of PIC. Particulate organic nitrogen (PON) was estimated to be equal to PN; that is it was assumed that all the PN was organic. Total silicon and aluminium content were determined by microwave digestion and inductively coupled plasma emission spectrometry using the facilities of the Woods Hole Oceanographic Institution and the methods described by *Bray et al.* [2000]. Biogenic silica was estimated from total silica by subtracting lithogenic silica estimated by assuming a lithogenic Al/Si mass ratio of 3.42 [*Taylor*, 1964]. Suspended particle studies during the SAZ Project support this use of Al as a proxy for lithogenic inputs [*Cardinal et al.*, this issue], and Cardinal et al. discuss possible uncertainties in this approach. For most samples, lithogenic silica made up a very small contribution of the total: <1% in the PFZ traps, 2-3% at the SAF, and 10-20% of the most silica-poor SAZ traps [*Bray et al.*, 2000]. The mass of lithogenic material in the samples was estimated from measured aluminium contents, assuming a crustal Al content of 84,000 ppm [*Taylor and McLennan*, 1985]. Contributions to the total mass flux from the silica and PIC components

Table 2. Sediment Trap Mooring Locations and Measured Currents

Site and Trap Designations	Latitude, °S	Longitude, °E	Bottom Depth, m	Trap Depth Below Surface, m	Mean Current Speed, cm s^{-1}	Maximum Current Speed, cm s^{-1}	Mean Current Direction,[a] deg
SAZ	46° 46'	142° 4'	4540				
47_1000				1060			
47_2000				2050	4.5	14.6	213
47_3800				3850	5.0	17.6	194
SAF	51° 0'	141° 44'	3780				
51_3100				3080	6.0	19.7	143
PFZ/PZ	53° 45'	141° 45'	2280				
54_800				830	8.3	22.6	107
54_1500				1580	4 8	18.5	106

[a] Current time series are available from *Bray et al.* [2000]

Table 3. Individual Cup Fluxes for <1 mm Fraction [a]

Cup	Sampling Period Mid Point	Length, days	Total Mass Flux, mg m^{-2} d^{-1}	Al Molar Flux, µmol m^{-2} d^{-1}	Si-Bio Molar Flux, µmol m^{-2} d^{-1}	PIC Molar Flux, µmol m^{-2} d^{-1}	POC Molar Flux, µmol m^{-2} d^{-1}	POC/PON Molar Ratio
47_1000								
1	Sept. 26, 1997	8.5	21	2.0[b]	36[b]	111	206	5.4
2	Oct. 04, 1997	8.5	36	3.3[b]	61[b]	238	201	6.9
3	Oct. 13, 1997	8.5	103	9.6	176	680	545	7.9
4	Oct. 21, 1997	8.5	127	12.1	183	876	550	7.5
5	Oct. 30, 1997	8.5	79	6.2	99	566	325	6.5
6	Nov. 07, 1997	8.5	53	3.9	54	401	217	7.5
7	Nov. 16, 1997	8.5	62	5.2	77	440	283	7.4
8	Nov. 24, 1997	8.5	10	0.7[b]	16[b]	73[b]	44[b]	7.2[b]
9	Dec. 03, 1997	8.5	10	0.7[b]	15[b]	70[b]	42[b]	7.2[b]
10	Dec. 11, 1997	8.5	12	0.8[b]	18[b]	88	48	7.1
11	Dec. 20, 1997	8.5	35	2.1	67	192	277	6.9
12	Dec. 28, 1997	8.5	132	6.9	513	461	1174	8.2
13	Jan. 04, 1998	4.25	87	5.8	219	479	623	7.2
14	Jan. 08, 1998	4.25	112	6.7	229	579	1027	7.0
15	Jan. 12, 1998	4.25	77	3.5	207	385	643	7.4
16	Jan. 16, 1998	4.25	43	1.7	96	244	308	6.9
17	Jan. 21, 1998	4.25	91	3.5	305	435	646	7.3
18	Jan. 25, 1998	4.25	116	4.4	390	545	880	7.1
19	Jan. 31, 1998	8.5	161	4.3	836	466	1418	7.9
20	Feb. 09, 1998	8.5	10	0.3[b]	51[b]	29[b]	87[b]	7.9[b]
21	Feb. 17, 1998	8.5	0	0	0	0	0	
47_2000								
1	Sept. 26, 1997	8.5	21	1.6	34	124	155	7.4
2	Oct. 04, 1997	8.5	31	2.5	47	200	167	6.8
3	Oct. 13, 1997	8.5	59	5.5	87	363	370	6.3
4	Oct. 21, 1997	8.5	98	8.8	156	702	337	7.3
5	Oct. 30, 1997	8.5	92	8.6	134	667	307	8.0
6	Nov. 07, 1997	8.5	68	7.6	77	509	202	8.0
7	Nov. 16, 1997	8.5	91	13.0	112	682	248	7.7
8	Nov. 24, 1997	8.5	76	12.8	90	561	216	7.3
9	Dec. 03, 1997	8.5	65	10.1	91	465	244	7.8
10	Dec. 11, 1997	8.5	65	8.3	125	403	349	8.4
11	Dec. 20, 1997	8.5	82	12.0	137	562	282	8.0
12	Dec. 28, 1997	8.5	132	14.7	375	771	605	8.4
13	Jan. 04, 1998	4.25	197	17.4	746	1019	890	8.2
14	Jan. 08, 1998	4.25	187	13.6	591	1017	913	7.9
15	Jan. 12, 1998	4.25	218	13.2	797	1158	1100	8.3
16	Jan. 16, 1998	4.25	149	9.0	539	792	685	7.7
17	Jan. 21, 1998	4.25	145	6.7	653	704	698	7.8
18	Jan. 25, 1998	4.25	156	7.0	624	785	726	8.2
19	Jan. 31, 1998	8.5	214	8.8	1117	840	1280	7.9
20	Feb. 09, 1998	8.5	142	3.5	761	491	933	7.5
21	Feb. 17, 1998	8.5	0	0	0	0	0	
47_3800								
1	Sept. 26, 1997	8.5	18	2.1	33	130	45	7.8
2	Oct. 04, 1997	8.5	23	2.3	37	161	84	7.1
3	Oct. 13, 1997	8.5	25	2.6	35	174	91	6.9
4	Oct. 21, 1997	8.5	59	6.6	88	427	188	7.9
5	Oct. 30, 1997	8.5	51	5.2	63	353	299	9.2
6	Nov. 07, 1997	8.5	66	9.2	83	481	207	7.7
7	Nov. 16, 1997	8.5	74	11.4	78	564	192	7.2
8	Nov. 24, 1997	8.5	37	6.0[b]	42[b]	260	179	7.9
9	Dec. 03, 1997	8.5	38	6.4	46	284	108	8.0
10	Dec. 11, 1997	8.5	72	12.7	79	533	194	8.5
11	Dec. 20, 1997	8.5	43	5.6	45	321	132	6.8
12	Dec. 28, 1997	8.5	86	8.7	233	498	421	7.8
13	Jan. 04, 1998	4.25	60	7.0	100	411	223	8.4

Table 3. (continued)

Cup	Sampling Period Mid Point	Length, days	Total Mass Flux, mg m^{-2} d^{-1}	Al Molar Flux, µmol m^{-2} d^{-1}	Si-Bio Molar Flux, µmol m^{-2} d^{-1}	PIC Molar Flux, µmol m^{-2} d^{-1}	POC Molar Flux, µmol m^{-2} d^{-1}	POC/PON Molar Ratio
14	Jan. 08, 1998	4.25	70	6.7	188	424	280	8.5
15	Jan. 12, 1998	4.25	120	11.9	331	735	451	8.1
16	Jan. 16, 1998	4.25	135	13.1	346	841	472	8.5
17	Jan. 21, 1998	4.25	105	8.0	351	594	407	7.9
18	Jan. 25, 1998	4.25	116	8.3	457	628	452	8.1
19	Jan. 31, 1998	8.5	109	8.8	389	548	489	8.2
20	Feb. 09, 1998	8.5	186	8.5	840	785	1092	7.8
21	Feb. 17, 1998	8.5	141	10.5	527	702	747	8.0
51_3100								
1	Sept. 26, 1997	8.5	98	2.6	720	260	413	7.1
2	Oct. 04, 1997	8.5	121	2.8	566	561	534	7.9
3	Oct. 13, 1997	8.5	217	3.4	583	1461	596	7.5
4	Oct. 21, 1997	8.5	279	5.3	597	2001	683	7.4
5	Oct. 30, 1997	8.5	225	4.5	521	1600	517	7.1
6	Nov. 07, 1997	8.5	263	3.7	420	2137	315	6.8
7	Nov. 16, 1997	8.5	166	3.9	537	1088	254	5.8
8	Nov. 24, 1997	8.5	226	4.0	954	1334	406	6.9
9	Dec. 03, 1997	8.5	107	2.2	464	600	215	7.3
10	Dec. 11, 1997	8.5	40	1.5	117	210	94	6.3
11	Dec. 20, 1997	8.5	123	4 2	743	552	206	7.0
12	Dec. 28, 1997	8.5	92	3.6	543	446	139	6.7
13	Jan. 04, 1998	4.25	60	2.4	266	341	118	6.6
14	Jan. 08, 1998	4.25	71	2.8	400	348	130	6.6
15	Jan. 12, 1998	4.25	87	2.9	527	387	165	7.3
16	Jan. 16, 1998	4.25	99	3.7	716	401	196	7.7
17	Jan. 21, 1998	4.25	108	7.4	747	435	205	7.5
18	Jan. 25, 1998	4.25	169	5.5	1358	540	339	7.2
19	Jan. 31, 1998	8.5	164	5.1	1235	521	372	7.4
20	Feb. 09, 1998	8.5	170	6.1	1249	644	291	6.8
21	Feb. 17, 1998	8.5	177	8.0	1263	712	285	6.9
54_800								
1	Sept. 26, 1997	8.5	3	0.0[b]	24[b]	7[b]	6[b]	6.2[b]
2	Oct. 04, 1997	8.5	12	0.2[b]	102[b]	31[b]	28[b]	6.2[b]
3	Oct. 13, 1997	8.5	12	0.2[b]	102[b]	31[b]	28[b]	6.2[b]
4	Oct. 21, 1997	8.5	47	0.8	417	126	114	6.2
5	Oct. 30, 1997	8.5	100	0.9	875	260	229	5.6
6	Nov. 07, 1997	8.5	142	0.7	1321	355	189	5.7
7	Nov. 16, 1997	8.5	233	1.0	2193	564	358	5.5
8	Nov. 24, 1997	8.5	166	0.8	1360	458	363	5.6
9	Dec. 03, 1997	8.5	53	0.2	218	205	198	5.7
10	Dec. 11, 1997	8.5	63	0.1	342	165	205	5.4
11	Dec. 20, 1997	8.5	148	0.4	1062	265	419	5.7
12	Dec. 28, 1997	8.5	112	0.1	646	297	381	5.7
13	Jan. 04, 1998	4.25	110	0.5	852	295	412	6.8
14	Jan. 08, 1998	4.25	100	0.5	902	230	375	6.6
15	Jan. 12, 1998	4.25	152	0.4	1543	286	334	5.8
16	Jan. 16, 1998	4.25	153	0.7	1461	314	479	6.5
17	Jan. 21, 1998	4.25	265	1.3	2741	505	730	7.0
18	Jan. 25, 1998	4.25	396	2.9	4315	659	823	6.3
19	Jan. 31, 1998	8.5	276	0.9	2858	471	580	6.2
20	Feb. 09, 1998	8.5	142	0.4	1237	370	384	5.3
21	Feb. 17, 1998	8.5	66	0.4	508	204	189	5.6
54_1500								
1	Sept. 26, 1997	8.5	21	0.5	191	49	45	7.0
2	Oct. 04, 1997	8.5	21	0.5	191	49	45	7.0
3	Oct. 13, 1997	8.5	31	0.7	256	94	64	7.2
4	Oct. 21, 1997	8.5	31	0.7	256	94	64	7.2
5	Oct. 30, 1997	8.5	39	0.8	342	110	78	5.9

Table 3. (continued)

Cup	Sampling Period Mid Point	Length, days	Total Mass Flux, mg m^{-2} d^{-1}	Al Molar Flux, μmol m^{-2} d^{-1}	Si-Bio Molar Flux, μmol m^{-2} d^{-1}	PIC Molar Flux, μmol m^{-2} d^{-1}	POC Molar Flux, μmol m^{-2} d^{-1}	POC/PON Molar Ratio
6	Nov. 07, 1997	8.5	71	0.9	577	192	119	6.2
7	Nov. 16, 1997	8.5	93	1.1	826	245	142	6.3
8	Nov. 24, 1997	8.5	129	1.0	1149	319	215	5.8
9	Dec. 03, 1997	8.5	135	0.8	1025	455	178	5.7
10	Dec. 11, 1997	8.5	184	0.9	1783	426	287	6.5
11	Dec. 20, 1997	8.5	252	0.9	2601	435	422	6.3
12	Dec. 28, 1997	8.5	153	1.1	1450	269	367	6.3
13	Jan. 04, 1998	4.25	85	0.7	814	157	231	7.0
14	Jan. 08, 1998	4.25	92	0.7	907	160	269	7.0
15	Jan. 12, 1998	4.25	131	0.9	1304	179	320	7.8
16	Jan. 16, 1998	4.25	84	0.6	839	117	233	7.2
17	Jan. 21, 1998	4.25	81	0.7	568	132	195	7.8
18	Jan. 25, 1998	4.25	116	0.8	1254	151	232	7.1
19	Jan. 31, 1998	8.5	81	0.5	818	112	167	6.9
20	Feb. 09, 1998	8.5	47	0.3	511	56	84	6.9
21	Feb. 17, 1998	8.5	34	0.3	346	55	59	8.1

[a] Mass fluxes listed as zero were too small to measure (<1 mg).

[b] Component fluxes representing intervals for which insufficient material was available for component measurements and were estimated from measured mass fluxes and the average compositions of adjacent cups.

were estimated assuming compositions of SiO_2 and $CaCO_3$. For simplicity, the mass flux contribution given for POC is that of carbon alone, converting this to a particulate organic matter mass flux assuming a particular composition, e.g., $C_{106}H_{175}N_{16}O_{42}P$, [*Anderson*, 1995] would increase the calculated organic mass flux by a factor of ~1.8. For all measured components, analytical uncertainties (detailed by *Bray et al.* [2000]) were much less than those of the sample-splitting process (which introduced variations among the masses of different splits of ~8% for these samples [*Bray et al.*, 2000]).

Thorium 230 was extracted by total digestion (along with ^{229}Th added as a yield tracer), purified by ion exchange chromatography, and measured by inductively coupled mass spectrometry following the methods outlined by *Choi et al.* [2001]. The amount of "excess" ^{230}Th scavenged from the water column ($^{230}Th_{ex}$) was calculated by subtracting the small radiogenic contribution at secular equilibrium from particulate lithogenic ^{238}U (lithogenic ^{238}U estimated from measured ^{232}Th and an average crustal $^{238}U/^{232}Th$ activity ratio of 0.8±0.2).

On the basis of salinity measurements after recovery, loss of solution was minimal during the deployment, and therefore we have not made any corrections for loss of particulate or dissolved material [*Bray et al.*, 2000]. Solution-dissolved silicate and phosphate concentrations were well above those of the cup deployment solution (attempts to measure nitrate were foiled by inactivation of the cadmium reduction column, probably by the mercuric chloride trap poison). For the SAZ and PFZ traps the excess silica in solution generally represented 5-10% of the total (particulate+dissolved) with a few cups reaching 20%. In the SAZ, where particulate silica collections were much smaller, the solution typically contributed 20-30% of the total in the cups. Because we did not measure particulate phosphate and could not measure dissolved nitrate, a direct estimate of the solution contribution to these nutrient element fluxes was not possible. However, assuming a Redfield N/P (16) for the particles, the dissolved phosphate contribution to total phosphate appears to be quite large and variable, ranging from 10-80%, with typical values of ~20% in deep traps and ~40% in shallow traps [*Bray et al.*, 2000]. High dissolved phosphate levels have been observed previously [e.g. *Honjo and Manganini*, 1992; *von Bodungen et al.*, 1991], but the relative contributions from dissolution of <1 mm particles versus losses from large organisms are unknown. Because of this uncertainty, and to simplify comparisons with previous studies, we report here the <1 mm elemental and mass fluxes, without correction for dissolution or inclusion of the >1 mm fraction (which was dominated by sparse, macroscopic animals including small fish, coelenterates, and crustacea, for which a settling origin is uncertain [*Bray et al.*, 2000]). This simplification should be kept in mind in comparisons of nutrient element ratios among the traps and with surface water-dissolved and particulate values.

3. Results

3.1. Total Collected Fluxes for the Deployment Period

The total and major component mass fluxes for the six traps for the full 153 day collection period are shown in Figure 3 and listed in Table 4. Total mass flux was greatest in

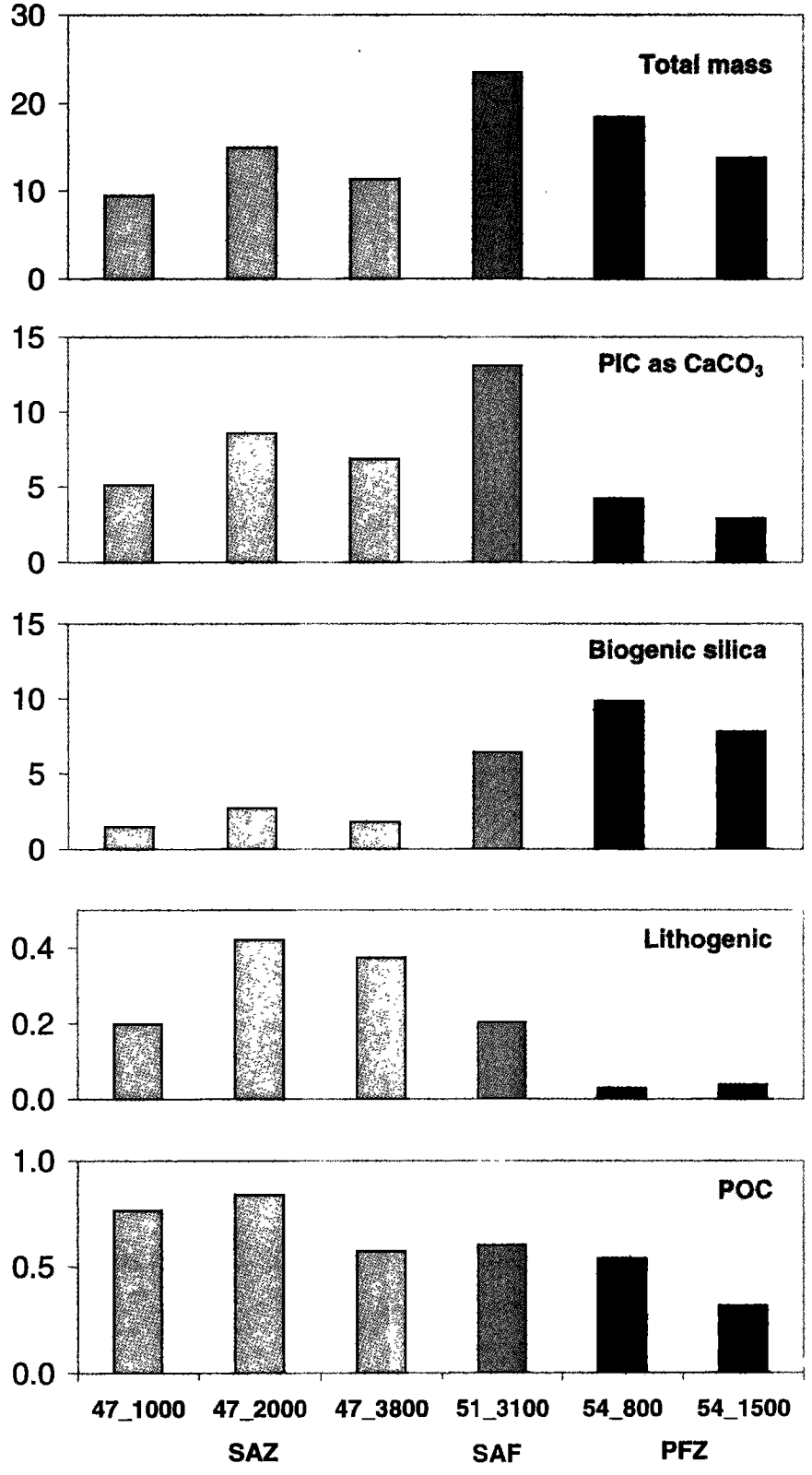

Figure 3. Total and major component mass fluxes for the <1 mm particulate fraction summed for the full collection period of 153 days from September 21, 1997, to February 21, 1998 (g m^{-2} (153 days)$^{-1}$).

the deep trap beneath the SAF, closely followed by the PFZ traps, with the lowest total flux collected in the SAZ. The total flux decreased with depth in the PFZ between 800 and 1500 m and in the SAZ between 2000 and 3800 m, but the shallowest SAZ trap near 1000 m exhibited a lower flux than the two deep traps. These relations with depth held true for all the major components.

PIC dominated the mass flux in the SAZ and beneath the SAF but contributed much less to PFZ export, which was dominated by biogenic silica. Despite the lower mass flux in

Table 4. Fluxes for <1 mm Fraction

Trap	Total Mass Flux	Lithogenic	SiO_2-bio	PIC as $CaCO_3$	POC	POC/PON Molar Ratio	$^{230}Th_{ex}$ Flux/Production, %
Fluxes Determined During Deployment Period, g m^{-2} (153 days)$^{-1}$							
47_1000	9	0.20	1.5	5.1	0.76	7.2	60
47_2000	15	0.42	2.7	8.6	0.84	7.8	50
47_3800	11	0.36	1.8	6.8	0.57	7.9	60
51_3100	24	0.20	6.4	13.1	0.60	7.0	110
54_800	18	0.03	9.8	4.2	0.53	6.0	70
54_1500	14	0.04	7.7	2.9	0.31	6.8	70
Estimated Annual Fluxes Assuming a Low Flux of 15 g m^{-2} yr^{-1} Outside the Collection Period for all Traps, g m^{-2} yr^{-1}							
47_1000	18	0.38	2.8	9.7	1.4		
47_2000	23	0.66	4.3	13.4	1.3		
47_3800	20	0.62	3.1	12.0	1.0		
51_3100	32	0.28	8.7	17.8	0.8		
54_800	27	0.04	14.3	6.2	0.8		
54_1500	22	0.06	12.5	4.7	0.5		

the SAZ the POC flux was similar to or greater than that observed in the traps farther south in the SAF and PFZ. The POC/PON molar ratio of the organic matter in all the traps ranged from 6 to 8, consistent with that of phytoplankton production (Table 4). The PFZ traps exhibited lower ratios (6.0 to 6.8) than the SAF and SAZ (7.2 to 7.9). There was a slight increase in POC/PON with depth among the SAZ traps (47°S), but this was not observed in the PFZ. Lithogenic material provided a negligible contribution (<1%) to the total mass flux in all the traps but was an order of magnitude higher in the SAZ and SAF than in the PFZ (Table 4).

It is reasonable to ask whether the shallowest SAZ trap (SAZ 47_1000) may have undercollected in comparison to the other SAZ traps. The current meter for this trap did not function, but currents measured at the site in the following year (T. W. Trull, unpublished data, 2001) were similar to those measured at 2000 m (Table 2). Thus there is no simple argument for possible undertrapping by the SAZ 47_1000 trap as a result of higher current velocity in comparison to the deeper SAZ 47 traps. Shallower traps (<1000 m), however, may undercollect at current velocities that do not affect deeper traps (>2000 m) because shallow particles may be less consolidated and more easily disrupted by the velocity fields surrounding trap funnels [*Honjo and Manganini*, 1993; *Yu et al.*, 2001]. We thus have attempted to constrain further the trapping efficiency of individual traps by comparing the intercepted flux of $^{230}Th_{ex}$ to its production in the water column above the trap [*Brewer et al.*, 1980]. The amounts of $^{230}Th_{ex}$ collected over the entire trap deployment, expressed as a percentage of production, are given in Table 4. They have uncertainties from splitting and analytical errors of ~10% (e.g., the SAZ 47_1000 trap collected 60±10% of the water column $^{230}Th_{ex}$ production). These percentages provide an indication of the efficiency of trapping, with 100% suggesting neither overcollection nor undercollection of $^{230}Th_{ex}$. The use of $^{230}Th_{ex}$ alone in the assessment of trap collection efficiency, however, does not permit the evaluation of horizontal transport of radionuclides by advection and eddy diffusion, which requires combining $^{231}Pa_{ex}$ and $^{230}Th_{ex}$ measurements [*Bacon et al*, 1985; *Bacon*, 1996; *Yu et al.*, 2001]. In regions characterized by shoaling isopycnals, such as the Antarctic Circumpolar Current (ACC), there is a lateral addition of $^{230}Th_{ex}$ [*Rutgers van der Loeff and Berger*, 1993], and thus trapping efficiencies estimated from $^{230}Th_{ex}$ flux, neglecting this lateral input, should be viewed as maximum estimates. We are pursuing the measurement of both $^{231}Pa_{ex}$ and $^{230}Th_{ex}$, including obtaining a full annual cycle from subsequent mooring deployments and the measurement of the distribution of these nuclides in surrounding water masses, to assess trap collection efficiencies in the future.

The available $^{230}Th_{ex}$ flux data, while suggesting some degree of undertrapping at 47° and 54°S, show no clear evidence for enhanced undertrapping at shallower depths (Table 4). It is thus possible that the vertical variations in the masses collected by the SAZ traps derive from the nature of particle settling in the ocean. Particles produced at the surface disperse laterally as they sink, and particles from source regions offset laterally from the trap site may bypass shallower traps but reach deeper traps as the lateral dispersion increases with depth [*Siegel et al.*, 1990]. In addition, vertical collection variations can result from mesoscale variations in surface particle production, because sediment traps collect from a relatively small specific area within a large "statistical funnel" [*Siegel and Deuser*, 1997].

Alternatively, the two lower SAZ traps (47_2000 and 47_3800) could have experienced lateral inputs that occurred below the depth of the shallower trap (47_1000). In that regard there are bathymetric highs along the Southeast Indian Ridge and Tasman Rise that reach up to 2000 m (but not 1000 m), although these features are relatively distant from the SAZ trap site (Figure 1). The two lower traps exhibited greater increases in lithogenic mass flux in comparison to the 1000 m trap than they did in biogenic components (Table 4), which could be taken to indicate a possible input from resuspended sediments. Some evidence for horizontal supply of particles at mesopelagic depths (0-600 m) has been found farther north (45°S) in this area [*Cardinal et al.*, this issue].

Because of the large uncertainties associated with estimating trapping efficiency from $^{230}Th_{ex}$ alone, we have not attempted to normalize our measured fluxes. Nonetheless, the

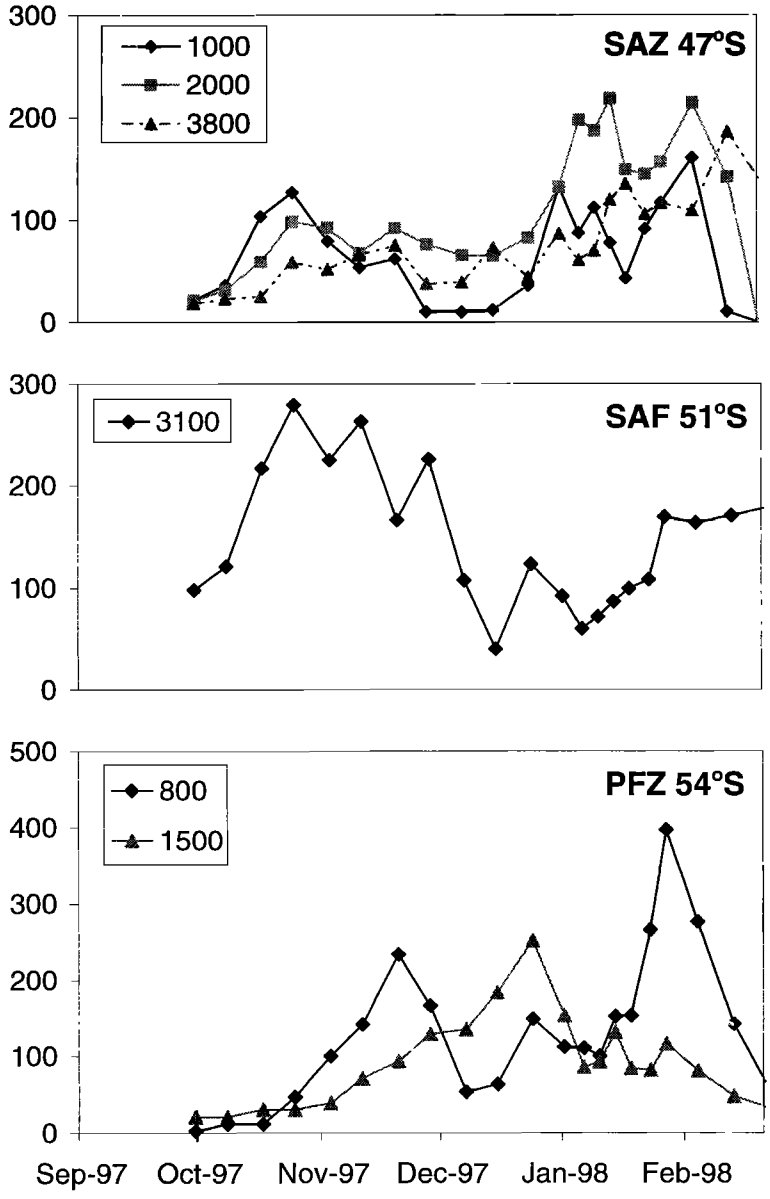

Figure 4. Seasonal record of total mass fluxes (mg m^{-2} d^{-1}).

$^{230}Th_{ex}$ results suggest that the SAZ and PFZ traps can be compared on an equal footing, with trap collection variations presenting only a minor aspect of latitudinal flux variations. In contrast, the higher $^{230}Th_{ex}$ collection in the SAF trap (Table 4) suggests that either trap collection efficiency was higher at this site or that particle focusing occurred and thus comparisons of the SAF trap with the SAZ and PFZ traps should be made with caution.

3.2. Seasonal Variations in Total and Component Fluxes

The cup-by-cup record of mass flux for each trap is shown in Figure 4. All of the traps obtained low total mass fluxes at the start of the deployment in early spring in September 1997. With the exception of the PFZ trap at 1500 m all the traps clearly exhibit two periods of enhanced export, in late spring and late summer, separated by a period of lower flux. The second, late summer, export period has greater amplitude than the spring period for all the traps, with the exception of the SAF trap (51_3100). The relatively shallow traps (47_1000, 47_2000, 54_800, and 54_1500) show a return to low fluxes at the end of the collection period, but this is not true for the deep traps (47_3800 and 51_3100), suggesting that the end of the seasonal export cycle had not yet reached these depths. This could also possibly explain the single export peak observed in the PFZ trap at 1500 m, if it is hypothesized that a second export peak occurred after the end of the deployment. This possibility is suggested by the similar shape and composition of the spring export peaks in the shallow (54_800) and deep (54_1500) PFZ traps, which suggest a lag in the arrival of the spring peak to the deep trap of about 5 weeks, sufficient to prevent the collection of the second late summer peak in the deep trap, and implies a settling rate of ~20 m d^{-1}. This settling rate is within the range of previous estimates [*Asper*, 1987; *Honjo*, 1996; *Pilskaln et al.*, 1998]. This view must be tempered by the fact that peak matching to infer settling rates is fraught with uncertainties, and a

particularly cautionary note has been provided by the recent reanalysis of the more than 10 year record of biweekly collections near Bermuda, which found no temporal lag between peak fluxes at 500 and 3200 m [*Conte and Ralph*, 1999].

There were clear seasonal changes in the nature of the collected material in the SAZ as shown in Figure 5. PIC dominated the flux of hard materials in the spring export peak, but in late summer, biogenic silica increased in importance, surpassing that of PIC toward the end of the deployment period. This temporal evolution was even more pronounced beneath the SAF (trap 51_3100). In contrast, there was little change in the relative fluxes of PIC and biogenic silica in the PFZ, which was dominated by silica throughout the deployment period. The small flux of lithogenic material showed a seasonal pattern very similar to the total mass flux at all the sites (Figure 6). The POC/PON ratio of the settling organic matter did not show any appreciable seasonal change (Table 3).

This seasonal pattern observed in our traps was somewhat different from recent results from the AESOPS program for SAZ and PFZ waters along 170°W (Figure 7) [*Honjo et al.*, 2000]. In the SAZ the time of initiation of significant export in spring was similar at the two longitudes, but the low flux period observed south of Australia was not observed along 170°W. In the PFZ the late summer flux magnitudes were similar at the two longitudes, but the spring export period observed south of Australia was not observed along 170°W. A spring (November) export peak was also found for Subantarctic waters near the Chatham Rise east of New Zealand, but with only a very subsidiary second export peak in late summer [*Nodder and Northcote*, 2001]. These differences are important and should provide useful constraints on the controls on export in the Southern Ocean, but a more detailed comparison is not possible here.

3.3. Annual Flux Estimates

To enable comparisons with other sites, annual flux estimates are also provided in Table 4. These were obtained by assuming that total mass flux outside the collection period was constant for all the traps (at 15 g m^{-2} yr^{-1}, Table 4, which is similar to the lower individual cup fluxes obtained during the collection period; Table 3), and this flux had the same compositions as the mean values obtained during the collection period (Table 4). This approach is justified by the decrease in fluxes at the end of the collection period for most traps (Figure 4) and the seasonal variations during the full annual collections in the AESOPS traps (Figure 7) but to a lesser degree by the seasonal cycle of biomass accumulation, which shows that significant levels do persist through March (Figure 8b). It is nonetheless an approximation, and the annual estimates in Table 4 should be viewed with caution.

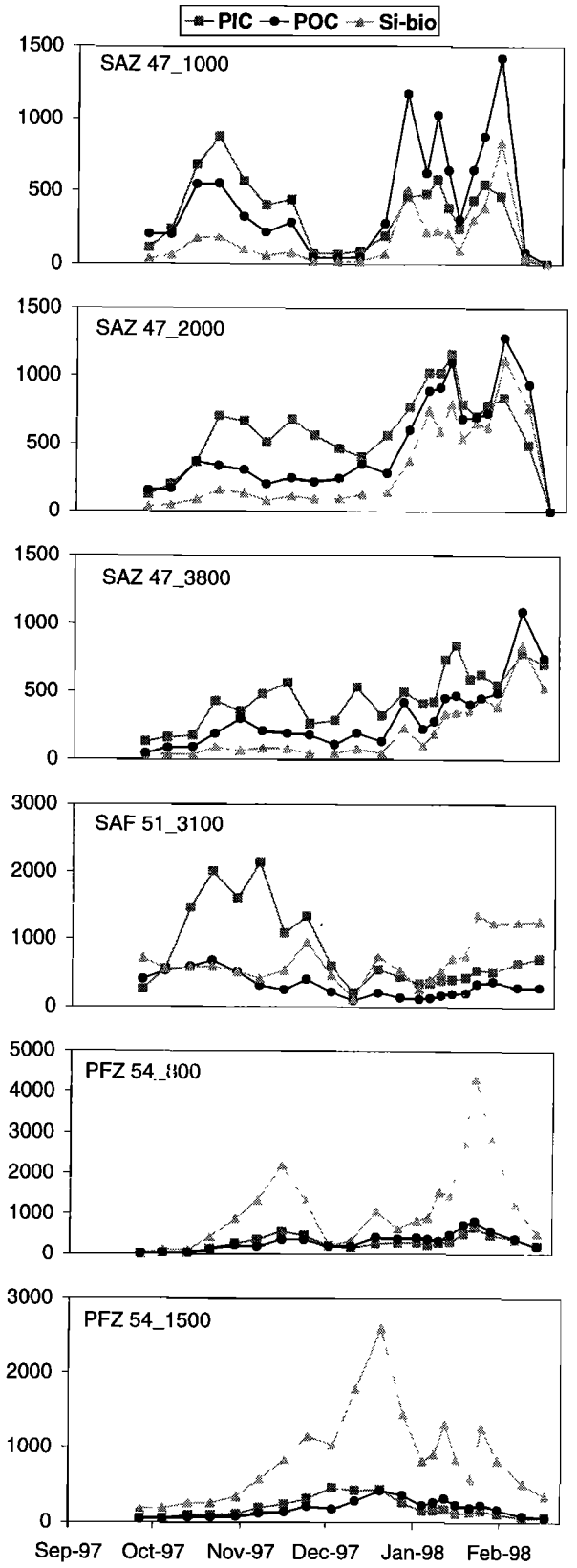

Figure 5. Seasonal record of major component fluxes (μmol m^{-2} d^{-1}).

4. Discussion

There are several simple questions that need clear answers in order for these particle flux measurements to advance our understanding of the Southern Ocean's role in the redistribution of carbon within the ocean and in the control of atmospheric carbon dioxide levels via the maintenance of low surface partial pressures of CO_2. (1) Can the fluxes measured in 1997-1998 be taken as typical? (2) To what region do they apply: entire circumpolar zones, the Australian sector, or a more reduced area? (3) Which zone, the SAZ or PFZ, is the more important zone for carbon export, not only in terms of magnitude but also in terms of its subsequent isolation from the atmosphere? (4) Is carbon export controlled primarily by

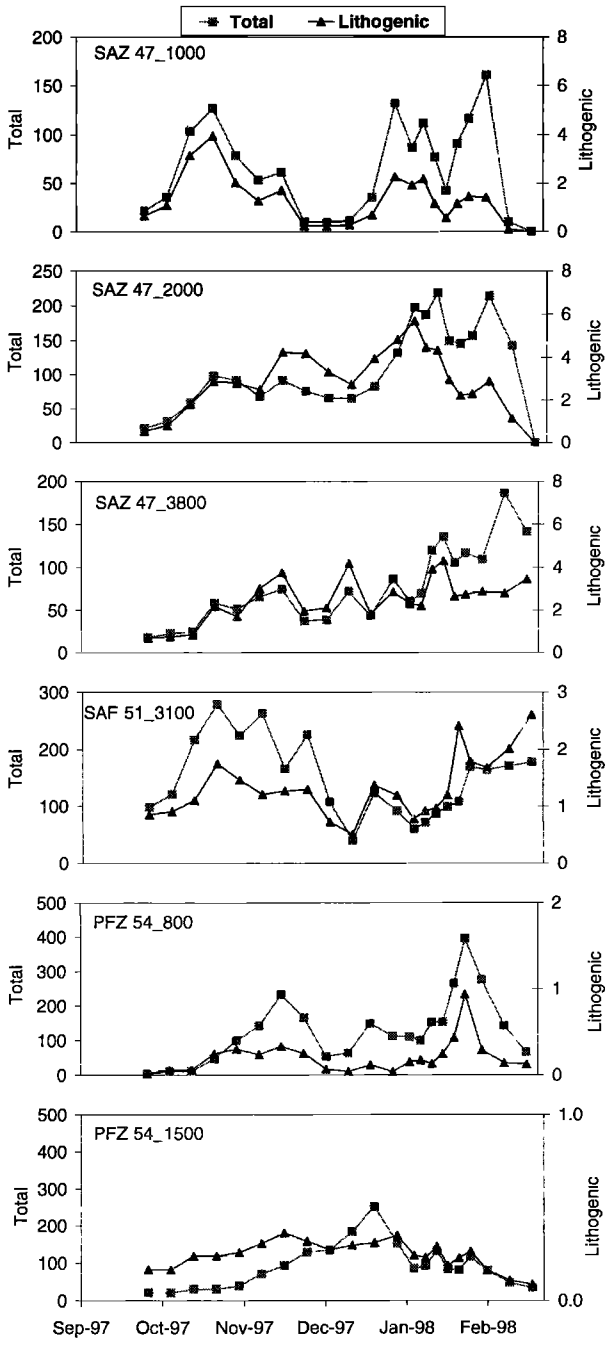

Figure 6. Seasonal record of total mass and lithogenic mass fluxes (mg m^{-2} d^{-1}).

the magnitude of primary production or by the fraction that escapes the surface food web and is exported to depth? (5) Is the magnitude and fate of exported carbon in the Southern Ocean important on a global scale, and is it strongly susceptible to climate change on the timescales of glacial-interglacial changes and of anthropogenic forcing? Obviously, this single study cannot answer all these questions in even a rudimentary way, but we can identify a few small contributions from the results.

4.1. Representativeness of the Measured Fluxes Collection Period

It is quite possible that the measured fluxes are not representative of a typical year. Figure 8a shows the seasonal evolution of sea surface temperature (SST) in this region. The 1997-1998 summer was exceptionally cool; SST averaged for SAZ waters near the traps showed a typical slow increase from typical winter temperatures until the start of summer in late December 1997, but then, in contrast to more typical years (the two shown are typical of the past 10 years), no further warming occurred, and the maximum temperature reached was more than 1°C lower than in most of the last 10 years. This cool summer condition also applies to the SAF and PFZ sites (Figure 8a), and appears to result from deep mixing induced by windy conditions rather than reduced insolation from cloudiness (the National Centers for Environmental Prediction (NCEP) climatology for this year estimates relatively high wind stresses in January and February but fairly typical insolation [*Kalnay et al.*, 1996]). The influence of deep mixing on production is not understood for these regions; both increases and decreases are possible. Deep mixing can reduce mean light levels thereby slowing production but can also bring limiting nutrients (either silica or iron in these regions) to the surface [*Parslow et al.*, this issue]. Interestingly, the timing of the cool summer period corresponds with the period of low flux to the shallow (~1000 m) traps that occurred midseason (Figures 4 and 5). However, if the cool summer did reduce production in midseason, there is some evidence to suggest that this did not limit the overall seasonal export as the extent of surface nutrient depletion at the time of trap recovery in March 1998 was very similar to that in March 1994 [*Lourey and Trull*, this issue], a year that experienced a more typical seasonal warming, as shown in Figure 8a. Only further measurements of export can address the representativeness of the 1997-1998 record. To give an idea of possible variations, annual POC fluxes at 1000 m depth in the northeast subarctic Pacific varied by nearly a factor of 3 over a 7 year record, with a relative standard deviation of ~50% [*Wong et al.*, 1999]; similar variability is evident in the shorter records for the Southern Ocean in Table 1.

4.2. Representativeness of the Measured Fluxes: Regional Oceanography

There are several aspects to assessing the regional representativeness of the SAZ, SAF, and PFZ moored trap sites. In terms of oceanographic structure the moorings lie just at the east end of a wide span of longitudes (from at least 90° to 145°E) over which the major fronts are approximately parallel and zonally aligned [*Olbers et al.*, 1992]. Farther to the west (beyond 80°E), in the central Indian Ocean sector, the SAZ is displaced northward in comparison to the region south of Australia, and surface waters are considerably warmer, although they display a similar seasonal cycle in pCO_2 [*Metzl et al.*, 1999]. The 80°E longitude also marks the upstream influence of the Kerguelen Plateau on the position and structure of the PFZ, and this region is known to experience elevated levels of algal biomass, perhaps in response to iron inputs from shelf waters [*Blain et al.*, 2000; *Bucciarelli et al.*, 2001; *Comiso et al.*, 1993]. To the east of the moorings, near 145°E, the ACC turns southeast, guided by the topography of the Southeast Indian Ridge, and the SAF and PF are found nearly 5° of latitude farther south at 170°E [*Olbers et al.*, 1992]. To the extent that temperature and seasonal light levels and day lengths force export, these waters are likely to behave differently from those south of Australia. The impingement of the ACC on the SE Indian

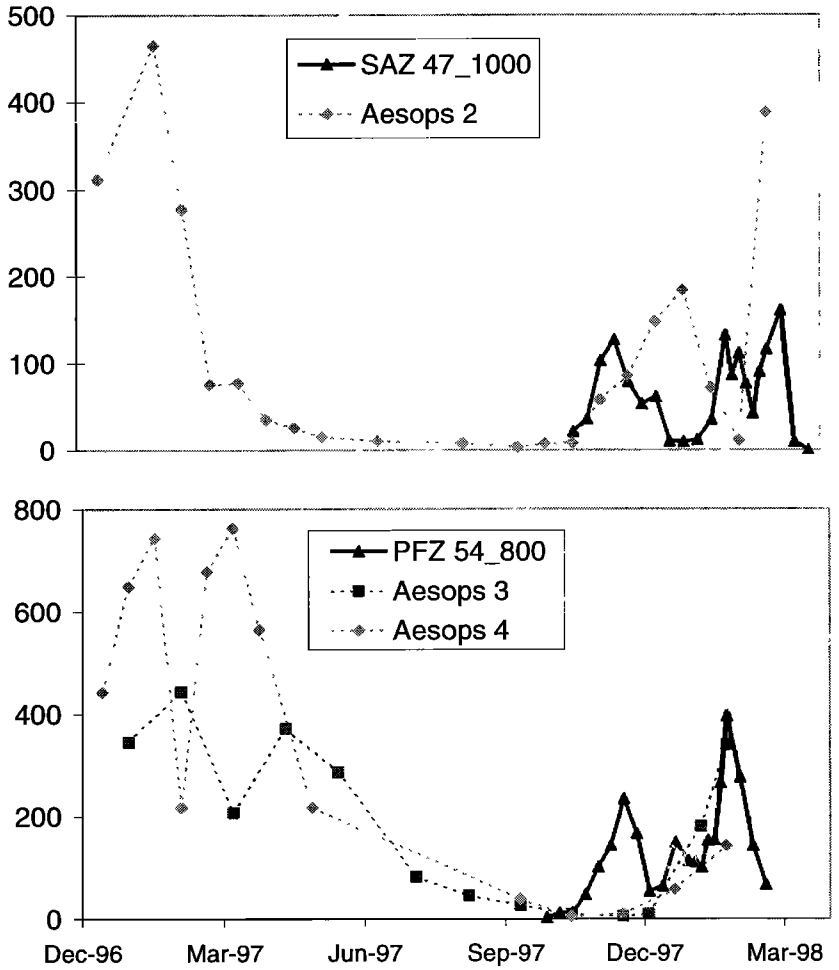

Figure 7. Comparison of SAZ Project and AESOPS *program* particle flux records for the SAZ and PFZ (total mass fluxes in mg m^{-2} d^{-1} for the shallowest traps at each site, all at ~1000 m except SAZ 54 at ~800 m). Locations of the moorings are shown in Figure 1. The comparisons should be viewed with caution because of oceanographic differences between the sites, for example for the SAZ comparison the AESOPS mooring 1 may have undercollected in response to high currents, and mooring 2 was very close to the SAF, and for the PFZ comparison, sea ice occasionally overlies AESOPS mooring 4 but never occurs at SAZ Project site PFZ 54.

Ridge is probably also the source of increased eddy variability downstream [*Morrow et al.*, 1994], which may also contribute to different production and export regimes [*Letelier et al.*, 1997; *Mcgillicuddy et al.*, 1995].

Thus there are good reasons to believe that oceanographic conditions differ from the studied region to the west beyond 90°E and to the east beyond 145°E. Within this region the SAZ and PFZ appear to be relatively homogeneous, albeit with some special characteristics. The Polar Front (PF) in this region can be thought of as having two branches, in that the "sub surface expression" of the front, taken as the most northerly extent of the subsurface temperature minimum (the 2°C isotherm at 200 m) occurs at 53°-54°S , while the "surface expression" of the front (in the form of the deepening of the temperature minimum layer) is much farther south at ~59°S. This has led to the definition of an Interpolar Frontal Zone in this region [*Parslow et al.*, this issue]. In relation to these features the 54°S mooring lies near to or north of the PF as defined by the presence of the subsurface temperature minimum (the PF shown in Figure 1). Of course, the locations of these features are not static, and large meanders, eddies, filaments, and divisions of the ACC flow associated with the PF and SAF are common [*Gille*, 1994; *Moore et al.*, 1999; *Morrow et al.*, 1994; *Phillips and Rintoul*, 2000]. The hydrographic section obtained at the time of trap recovery in March 1998 shows that a temperature minimum layer was present over the 54°S mooring site, though somewhat deeper than the 200 m definition for the PF (Figure 2). This is fairly typical, at least as judged from comparison to recent seasonal expendable bathythermograph and conductivity-temperature-depth sections in the vicinity [*Parslow et al.*, this issue; *Rintoul et al.*, 1997; *Rintoul and Trull*, this issue].

There are other aspects of the mooring sites that may influence the degree to which they can be considered representative of the zonal SAZ, SAF, and PFZ between 90° and 145°E. The SAZ experiences a weak recirculation in the region south of Tasmania, with waters in the northern half (between ~43° and ~46°S) flowing to the west, while waters in the southern half (between ~47° and 50°S) flow to the east along with the SAF waters and the rest of the ACC [*Rintoul and Sokolov*, 2001; *Rintoul and Trull*, this issue]. The SAZ 47 mooring is south of this recirculation and experienced east flowing circumpolar currents throughout the deployment

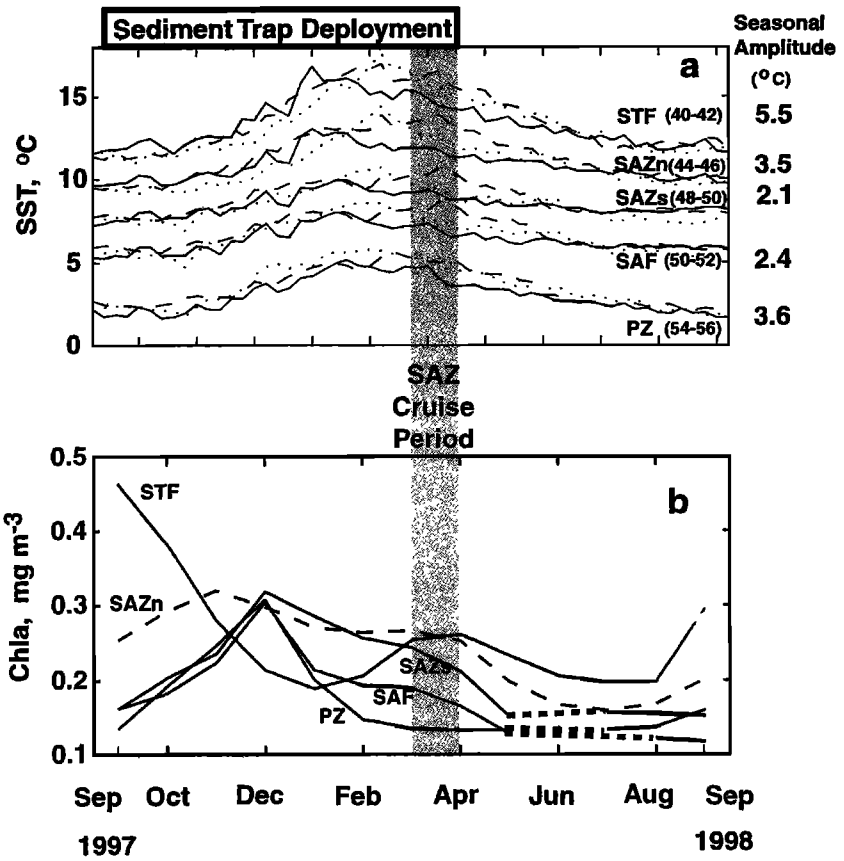

Figure 8. (a) Seasonality of sea surface temperature (SST) [*Kalnay et al.*, 1996], averaged in the 2° latitude bands marked on the plot, from 135 to 143°E. Solid lines are for the 1997-1998 year, which included the deployment period (marked by the bar at top). The preceding year is represented by dotted lines and was similar to the 10 year average for 1989-1999. The dashed lines represent the 1992-1993 year for which surface water nitrate depletion in the SAZ was very similar to the trap deployment year [*Lourey and Trull*, this issue]. The seasonal thermal amplitudes of the 1997-1998 deployment year for the different bands are given at the right. The southern SAZ experiences considerably lower seasonal warming than the northern SAZ because of SAF meandering and trans-SAF transports in surface waters [*Rintoul and Trull*, this issue]. (b) Seasonality of Sea-viewing Wide Field-of-view Sensor (SeaWiFS) surface chlorophyll, averaged in the same way as the SST data from monthly composites. Data gaps from low winter insolation angles are marked by dotted lines. The southern SAZ, SAF, and PFZ all show single mid summer peaks, of progressively shorter duration with increasing distance south. In contrast, the northern SAZ exhibits two peaks, similar to but not as extreme as in subtropical waters. The period of the SAZ Project biogeochemistry and SAF meander survey cruises is marked. Bio-optical studies at this time suggest the SeaWiFS algorithm overestimates chlorophyll in SAZ waters by ~50% [*Clementson et al.*, this issue].

period (Table 2). The recirculation has been observed between 140° and 150°E, and may extend much farther west, in a series of gyres or a long recirculation loop throughout the SAZ south of Australia [*Rintoul and Sokolov*, 2001; *Rintoul and Trull*, this issue]. The westward flowing water in the northern half of the SAZ exhibits some influence of the admixture of subtropical waters from the Tasman Sea, but is, in general, only slightly modified in terms of *T-S* properties from the properties of the east flowing southern SAZ waters. In addition, much warmer waters from eddies of the East Australia Current are known to "leak" beneath Tasmania and enter the SAZ and Subtropical Front (STF) to its west [*Rintoul and Sokolov*, 2001; *Rintoul and Trull*, this issue; *Cresswell*, 2000]. The influence of these waters on production and export is not known.

Remote sensing of chlorophyll concentrations offers some insights. Figure 8b shows that the northern half of the SAZ in the deployment year displayed a rather different seasonal cycle than the southern SAZ. Comparison to the STF and Polar Zone (PZ) waters suggests the southern SAZ exhibits similar seasonality to ACC waters, with a single late summer peak in biomass, while the northern SAZ displays a mix between this pattern and the late winter and late summer twin-peaked characteristics of the temperate STF. Despite these differences in the seasonality of chlorophyll accumulation the northern and southern SAZ displayed similar amounts of seasonal nutrient depletion of surface waters at the time of trap recovery in March 1998 [*Lourey and Trull*, this issue]. There is some evidence for relatively homogeneous coupling of production with export in the 90°-145°E sector in that the combined Coastal Zone Color Scanner ocean color chlorophyll record for 1978-1986 (available at http://seawifs.gsfc.nasa.gov/SEAWIFS/IMAGES/GALLERY.html) shows little spatial variability, with the possible exception of slightly higher levels in the SAZ south of the Great Australian Bight (near 130°E). The mean chlorophyll

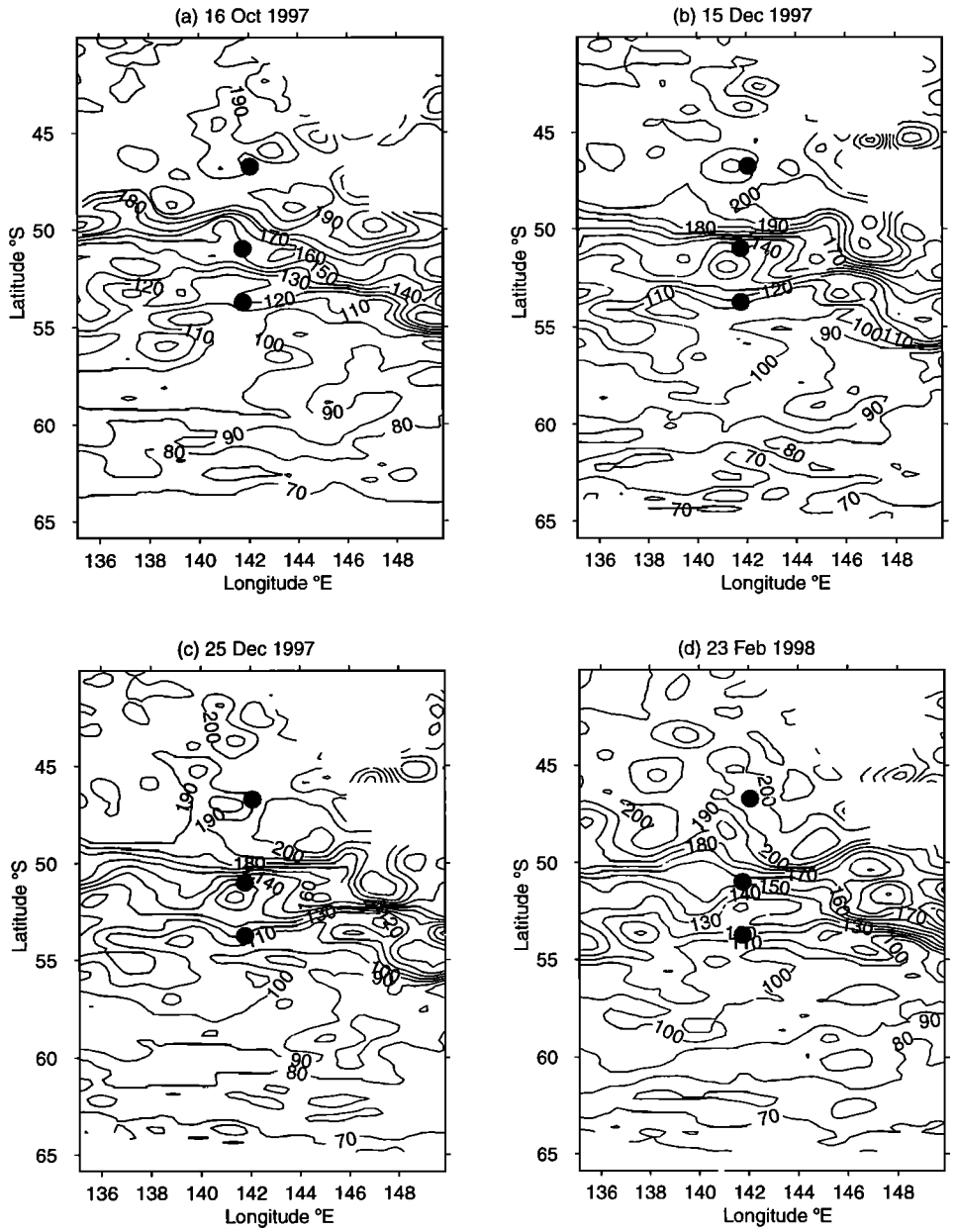

Figure 9. Selected sea surface height maps showing the extremes in meandering of the SAF. The maps were calculated from TOPEX/Poseidon anomalies combined with a climatology [*Olbers et al.*, 1992] using a reference depth of 2500 m. Height contours are at 10 cm intervals. The shallow Tasman Rise in the northeast corner of the images is not contoured because bathymetry is less than the reference level. The complexity of the ACC flow is visible in all the snapshots, which are marked by their dates. The SAZ 47 trap was always in a region of weak flows, usually well north of the SAF (marked by the closeness of the 170 and 180 cm contours between 50° and 51°S). The SAF occurred slightly to the north of the SAF 51 trap site during the deployment year (in contrast to previous estimations of its position, as shown in Figure 1). The PFZ 54 site was well south of the SAF, often near the 110-120 cm contours, which may mark slightly stronger flows associated with the PF. The large meander of the SAF examined during the SAZ Project meander survey in March 1998 (S. Rintoul, unpublished data, 2001) was already present in February and extended northeast toward the SAZ trap site (as marked by the 180 and 190 cm contours in Figure 9d). The SAF reached its farthest northward extent in early spring, as shown in Figure 9a, and its farthest southward position at midsummer, as shown in Figure 9b. At the time of low fluxes in all the traps (mid-December, Figures 4 and 5) the SAF was relatively zonal and near its average position, as shown in Figure 9c.

near the mooring sites appears to be very similar to conditions elsewhere within the 90°-145°E sector and does not show any influence of the elevated chlorophyll levels that occur to the east of Tasmania.

Thus it appears that the trap sites can be taken as representative of a relatively large region, the zonal SAZ, SAF, and PFZ from 90° to 145°E. The 1997-1998 year may not have been typical in terms of its seasonal progression (based on the SST record of Figure 8a), although there is some evidence that total seasonal export was nonetheless reasonably typical (based on the depletion of surface water nutrients [*Lourey and Trull*, this issue]). Given the propensity

for variations in the positions of the major zonal fronts (the SAF and PFZ), it is reasonable to ask whether changes in the positions of these fronts are likely to have influenced the seasonal record of export (Figures 4 and 5). In particular, the increase in the silica export in late summer in the SAZ raises the question as to whether this could reflect movement of the SAF northward over the SAZ mooring site. The short answer is that frontal movements do not appear to have been this extensive in the 1997-1998 year. Figure 9 shows the most northerly and southerly positions of the SAF during the deployment as revealed by contours of sea surface height obtained by combining TOPEX/Poseidon altimetry anomalies with a mean climatology with 2500 m reference depth [*Olbers et al.*, 1992]. The SAF remained at least 2° of longitude south of the SAZ trap site throughout the deployment. (The altimetry maps also reveal that the core of the SAF was always north of, though close to, the 51°S SAF mooring site and that the PFZ trap mooring at 54°S was always well south of the strong dynamic height gradient of the intense ACC flow.)

Given that all the traps exhibited the mid season (December 1997) low-flux period and that this was a time of essentially zonal, relatively steady structure and location of the SAF (Figure 9), it seems unlikely that the low flux was the result of SAF movements. A northward meander of the SAF in February and March 1998 did occur at the time of increasing silica export at the SAZ site, but the meander was still well south (more than 120 nm from the mooring, Figure 9). In addition, the carbon isotopic composition of POC in the SAZ traps was distinct from that of PFZ traps throughout the deployment period, arguing against supply of PFZ particles to the SAZ traps (M. Lourey and T. W. Trull, unpublished data, 2001). Overall, movements of the SAF and PFZ do not appear to have played a dominant role in controlling the seasonality of export at either the SAZ or PFZ sites but may have modulated the particle flux at the SAF site.

It is also possible that seasonal variations in the supply of silica and other nutrient-rich surface waters across the SAF in eddies, or within the surface layer, a process identified from hydrographic considerations [*Rintoul and Trull*, this issue], might have influenced the seasonality of export in the SAZ. At present we do not have knowledge of the seasonal variation in these processes. Their influence appears to be much greater in the southern SAZ than in the northern SAZ, as reflected in both the reduced amplitude of seasonal warming (Figure 8a) and the seasonal biomass accumulation (Figure 8b), yet both regions experience similar seasonal nutrient depletion [*Lourey and Trull*, this issue], and thus their influence on export also remains uncertain. Changes in the coupling of PFZ and SAZ production via this transport of surface nutrients across the SAF has recently been suggested as a possible explanation for glacial-interglacial timescale changes in apparent extents of nutrient utilization [*Sigman et al.*, 1999], and thus a better understanding of this process in the modern ocean would have benefits for climate change studies. While the seasonal variation in this process is unknown, both for the deployment period and in general, there is no reason to expect that the mooring region is unique in experiencing it. Overall, both the total exports and their seasonal development observed by the traps reasonably characterize the SAZ and PFZ for the 90° to 145°E sector of the Southern Ocean.

4.3. Relative Importance of the SAZ and PFZ to Carbon Export

The collected and estimated annual export of POC to 1000 m for the SAZ is larger than in the PFZ (Table 4 and Figure 3) and also rivals the SAF site (compare the two deep traps: SAZ 47_3800 and SAF 51_3100). This is despite the fact that the total fluxes of the PFZ and SAF exceed those of the SAZ. In short the particles in the SAZ were relatively POC rich. They were also slightly higher in PIC, as a fraction of total mass, in comparison to the PFZ. The export of PIC reduces the importance of POC export in terms of its influence on surface water carbon dioxide partial pressure because in seawater each mole of carbonate precipitation induces an ~0.6 mole increase in aqueous CO_2 concentration [*Frankignoulle et al.*, 1994], an effect that must be taken into account in assessing the relative contributions of physical and biological contributions to the seasonal cycle of pCO_2 in the SAZ [*Metzl et al.*, 1999]. In terms of the SAZ versus PFZ comparison, discounting the POC export by 0.6 times the PIC export (to provide an indication of the relative contributions to producing a chemically stratified ocean capable of keeping atmospheric pCO_2 low) increases the relative effectiveness of the SAZ in comparison to the PFZ because the PFZ actually had a higher ratio of PIC to POC (Table 4).

The collected fluxes are just a few percent of the materials that leave the surface as the majority of material is remineralized at mid depths. This is particularly true for POC, in comparison to biogenic silica, which dissolves relatively slowly, and PIC for which the lysocline depth in this region is ~3500 m [*Broecker and Takahashi*, 1978]. *Lourey and Trull* [this issue] have estimated the extent of seasonal nitrate and phosphate depletion of surface waters and the implied organic carbon export for both the trap deployment period (from winter through March 1998) and other years. For the deployment period the SAZ nitrate depletion was twice that of the PFZ, although phosphate depletion was only 20% higher, with the SAZ displaying a near-Redfield N/P depletion ratio (~15) much higher than that of the PFZ (~8). This suggests that the SAZ not only delivers more organic matter to the deep sea (as measured by the traps at 1000 m and deeper), which might have resulted from a difference in the extent of remineralization with depth, but that the SAZ also exports more organic matter to middepths than does the PFZ. Seasonal primary production, as estimated from ^{14}C uptake incubations in March 1998 and on several other cruises in the region (F.B. Griffiths, unpublished data, 2001), does appear to be higher in the SAZ than in the PFZ. Interestingly, this is the opposite pattern to that suggested by the accumulation of excess barite observed in March 1998, which was greater in the PFZ [*Cardinal et al.*, this issue]. There are several means of reconciling these differences, including uncertainties in the relationship between organic matter export and barite precipitation (particularly when comparisons are made between different algal communities, [*Cardinal et al.*, this issue, and references therein]) and the possibility that more extensive nutrient resupply through the summer export period occurs in the PFZ than in the SAZ, thereby reducing the apparent nutrient depletion in the PFZ [*Wang et al.*, this issue].

Comparing the POC collected by the traps with the apparent POC export based on seasonal nitrate depletion (assuming a Redfield C/N [*Lourey and Trull*, this issue]),

suggests that ~2% of the surface export reached the 1000 m trap in the SAZ and ~3% reached the 800 m trap in the PFZ. Given the uncertainties, these numbers are indistinguishable and do not imply a difference in the efficiency of deep export between the biogenic silica- dominated PFZ and the PIC-dominated SAZ. Both numbers are quite low in comparison to the relation [*Martin et al.*, 1987] expressing the flux at depth z as a function of that at 100 m depth:

$$J_z = J_{100m}(z/100)^{-0.858},$$

which predicts arrivals of 13 and 17% at 1000 and 800 m, respectively. The difference is probably less a reflection of the effectiveness of remineralization than it is a statement about the processes responsible for export. The *Martin et al.* [1987] expression relates the sinking particle flux at depth to the sinking particle flux just below the surface layer, whereas much of the surface nutrient depletion may occur via settling or deentrainment (i.e., the loss of suspended particles from the mixed layer when it shallows) of poorly aggregated materials that would not have been part of the sinking particle flux at 100 m as identified by sediment trap collections. This raises another important issue in assessing the effectiveness of export; sediment trap collections may not represent a large portion of the surface-exported materials. This problem is much greater in assessing export to middepths, of course, as biogenic-suspended particle concentrations do drop off strongly with depth [*Cardinal et al.*, this issue], but it does point to another possible reason for the discrepancy between midwater export proxies (such as excess barite) and deep sediment trap records.

The similarity of the SAZ and PFZ export fluxes of POC as a fraction of surface nutrient depletion are quite surprising. The SAZ and PFZ host dramatically different plankton communities, with large diatoms occurring more frequently and as a larger fraction of total phytoplankton biomass in the PFZ, while picoplankton and nanoplankton, particularly flagellates, dominate the SAZ (see Section 1 for references). Moreover, the presence of large phytoplankton, particularly diatoms, has been suggested as a key ecosystem component leading to relatively high export in comparison to total production [*Boyd and Newton*, 1999]. One possible explanation is that diatoms exported from the PFZ do not carry much POC with them. There is some support for this view in the observation of empty siliceous diatom tests at the time of trap recovery in March 1998 [*Kopczynska et al.*, this issue] and also in the trap data to the extent that the POC and PIC fluxes in the PFZ are highly correlated throughout the collection period, with little increase in POC flux accompanying the late summer biogenic silica export peak (Figure 5). Empty diatom tests have also been observed in the PFZ in the Atlantic sector [*Bathmann et al.*, 1997]. However, diatoms have been shown to dominate POC export in other PFZ studies [*Honjo et al.*, 2000], and other explanations, such as mesoscale repackaging processes or coincidental similarities, are possible for the correlations of Figure 5. Clearly, a better understanding of ecosystem control of export is required, in particular, to enable susceptibility to climate change to be evaluated. This includes both the mechanisms by which diatoms can promote high export (e.g., escape from grazing pressure, chain formation, and control of sinking rates) and the importance of the PIC-forming zooplankton (pteropods and foraminifera) that feed on them (see the references in Section 1).

From the perspective of carbon sequestration from the atmosphere the deep sediment trap fluxes are of greater import than materials that are remineralized at middepths because only those materials that are exported below the depth of the winter mixed layer are effectively removed. This is particularly important for the SAZ which experiences winter mixed layers in excess of 600 m [*Rintoul and Trull*, this issue], allowing the remineralized carbon to reequilibrate with the atmosphere. It is likely that this outgassing dominates over advective transport of the middepth accumulations of remineralized organic carbon into the ocean's interior because renewal of SAMW in this region appears to be quite slow (a residence time of 2-50 years has been estimated from CFC concentrations [*McNeil et al.*, this issue]). Winter mixed layers in the PFZ are not as deep but still reach to 150-200 m, and transport into the ocean interior by AAIW is probably similarly slow [*Rintoul and Bullister*, 1999]. For these reasons the POC export as measured in the traps is perhaps that which is most important, and the SAZ export slightly exceeds that of the PFZ. Once below 1000 m, the exported carbon is likely to remain at depth for centuries, before being slowly upwelled at lower latitudes [*Caldeira and Duffy*, 2000; *England*, 1995].

4.4. Contribution to Control of Atmospheric CO_2 and Susceptibility to Climate Change

Many studies have identified the Southern Ocean as particularly important to the control of atmospheric CO_2, both in terms of buffering of anthropogenic emissions and of long-term climate change (see the references in Section 1). The incremental results presented here do not change that overall picture, but they do emphasize the relatively large size of the "biological pump" in the SAZ and PFZ. The POC fluxes (g m^{-2} yr^{-1} at 1000 m depth) in the SAZ and PFZ obtained here (and in the other open Southern Ocean sites listed in Table 1) are larger than those of the equatorial Pacific, temperate North Atlantic, or northwest Pacific, though are exceeded by the monsoonal Arabian Sea (results summarized by *Honjo* [1997]) and similar to the global median (Table 1) estimated by *Lampitt and Antia* [1997]. Clearly, the high-nutrient, low-chlorophyll characteristics of the Southern Ocean should not be taken to indicate low activity or export.

Additional indications of the magnitude of the POC export in the SAZ are provided by comparison with air-sea fluxes of total and anthropogenic carbon dioxide. The seasonal export of organic carbon (3400±430 mmol m^{-2} for the same period as the trap collections) estimated from surface nitrate depletion [*Lourey and Trull*, this issue] is practically identical to the total air to sea transfer of carbon dioxide for the annual cycle (3220 mmol m^{-2} for 1995) obtained from pCO_2 measurements [*Metzl et al.*, 1999]. Thus carbon dioxide transferred from air to sea in the SAZ is rapidly carried below the seasonal thermocline; though, given the deep winter mixed layer, much of it is probably outgassed again. The total air-sea transfer is large, ~1 Gt C yr^{-1}, for the circumpolar SAZ [*Metzl et al.*, 1999], suggesting that variations in the fraction of this transfer, which is transported to depth by the biological pump could contribute to interannual variations in atmospheric CO_2 levels given that mean global net air-sea fluxes are ~1.5 Gt C yr^{-1} [*Keeling et al.*, 1995; *Lee et al.*, 1998]. In comparison to the storage rate of anthropogenic CO_2 in the SAZ south of Australia (as estimated from dissolved

inorganic carbon concentration changes over the past 30 years [*McNeil et al.*, this issue]), the SAZ surface export as estimated from nutrient depletion is ~10 times larger [*Lourey and Trull*, this issue]. Again, this suggests that variability in the biological pump can be significant in magnitude in comparison to other processes involved in CO_2 uptake in the ocean.

Susceptibility of carbon transports to climate change has many aspects, including response to changes in the global overturning circulation, direct temperature or radiation forcing of production, indirect forcing via changes in stratification on seasonal or weather timescales, supply of limiting trace nutrients from outside the ocean system (e.g., iron or nitrate), and variations in export efficiency driven by ecosystem structure (see Section 1 for references). The observation that south of Australia in 1997-1998, the SAZ exported similar or larger amounts of POC to 1000 m depth than did the PFZ, despite the greater presence of diatoms in the PFZ, is important. It challenges an emerging perspective on the ecosystem control of carbon export, that suggests that large phytoplankton, particularly diatoms, are a major aspect of efficient export [e.g., *Boyd and Newton*, 1999; *Buesseler*, 1998; *Laws et al.*, 2001; *Michaels and Silver*, 1988]. The observed high SAZ export may not be universal; indeed, the AESOPS program found greater POC export in the PFZ than in the SAZ (although it is probable that high currents reduced the trap collection efficiency at that SAZ site [*Honjo et al.*, 2000]). Nonetheless, the overall results of recent programs (Table 1) make it clear that the Southern Ocean exports a large amount of particulate carbon to the deep sea throughout its north-south extent and not just in high-productivity regions in the marginal ice zone or near the Polar Front.

5. Conclusions

The SAZ Project has provided the first measurements of deep sea sinking particle fluxes for the Australian sector of the Southern Ocean, with a particular focus on the SAZ and PFZ. Comparison with remote sensing and hydrographic results suggests these results are representative of the East Antarctic sector from 90° to 145°E but that the 1997-1998 period examined may have been unusual in that it experienced relatively low summer warming of surface waters. Continuing deployment of the SAZ Project moorings is underway to investigate interannual variability. Comparison of organic carbon export at ~1000 m depth suggests the SAZ exports slightly more than the PFZ, a view consistent with surface primary production and nutrient depletion observations but somewhat different than that suggested by the AESOPS program in the southwest Pacific sector along 170°W, which found the PF to be the region of greatest export [*Honjo et al.*, 2000]. This difference may reflect the north-south offsets of the zones at the two latitudes, or other factors, and offers an important opportunity for further comparisons. The SAZ Project and other recent sediment trap programs (Table 1) have demonstrated that organic carbon export in the Southern Ocean is large in comparison to many other regions of the global ocean.

Acknowledgments. The SAZ Project is grateful for logistical and equipment support from ANARE and the Australian Antarctic Division (T. Trull, ASAC grants 1156 and 2256), the CSIRO Division of Marine Research Oceans and Climate Program, the Australian Geological Survey Organisation (AGSO), and New Zealand's National Institute of Water and Atmospheric Research (NIWA). Support for T. Trull to perform ^{230}Th analyses at WHOI was provided by DIST. The officer, crews, and scientific staff of *Aurora Australis* voyages AA9701 and AA9706 are thanked for their professionalism and unflagging dedication in rough conditions. Neil White, Chris Rathbone, Kim Badcock, John Church, John Parslow, and Steve Rintoul of CSIRO provided key remote sensing support in near real time in the field and during analysis. Ian Helmond, Danny Mclauglin, Kevin Miller, and Mark Rosenberg designed, constructed, and deployed the moorings. Julie Palmieri (WHOI) and Neale Johnston (Antarctic CRC) performed the CHN and supernatant analyses, respectively. Thanks to Antarctic CRC scientists Pete Sedwick and Brian Griffiths for support in organizing the SAZ Project, Will Howard for trap deployments here and in New Zealand as part of equipment exchanges, Teresa O'Leary for help with sample splitting, and John Church and Gary Meyers of CSIRO for unflagging commitment to the project. Constructive reviews from C Pilskaln and an anonymous reviewer greatly improved the paper.

References

Accornero, A., A. Bergamasco, A. Monoco, and S. Tucci, Particle fluxes at the edge of the Ross Ice Shelf: The role of physical forcing, in *Oceanography of the Ross Sea, Antarctica*, edited by G. Spezie and G.M.R. Manzella, pp. 176-195, Springer-Verlag, New York, 1999.

Anderson, L., On the hydrogen and oxygen content of marine phytoplankton, *Deep Sea Res., Part I, 42*, 1675-1680, 1995.

Asper, V.L., Measuring the flux and sinking speed of marine snow aggregates, *Deep Sea Res., Part A, 34*, 1-17, 1987.

Bacon, M., Evaluation of sediment traps with naturally occuring radionuclides, in *Particle Flux in the Ocean*, edited by V. Ittekkot et al., pp. 85-90, John Wiley, New York, 1996.

Bacon, M.P., C.-A. Huh, A.P. Fleer, and W.G. Deuser, Seasonality in the flux of natural radionuclides and plutonium in the deep Sargasso Sea, *Deep Sea Res., Part A 32*, 273-285, 1985.

Bathmann, U.V., R. Scharek, C. Klaas, C.D. Dubischar, and V. Smetacek, Spring development of phytoplankton biomass and composition in major water masses of the Atlantic sector of the Southern Ocean, *Deep Sea Res., Part II, 44*, 51-67, 1997.

Bidigare, R.R., T.J. Frank, C. Zastrow, and J M. Brooks, The distribution of algal chlorophylls and their degradation products in the Southern Ocean, *Deep Sea Res., Part A, 33*, 923-937, 1986.

Blain, S. et al , A biogeochemical study of the island mass effect in the context of the Iron Hypothesis: Kerguelen Islands, Southern Ocean, *Deep Sea Res., Part I, 48*, 163-187, 2000.

Boyd, P W. and P. Newton, Does planktonic community structure determine downward particulate organic carbon flux in different oceanic provinces?, *Deep Sea Res., Part I, 46*, 63-91, 1999.

Boyd, P. et al., A mesoscale phytoplankton bloom in the polar Southern Ocean stimulated by iron fertilization, *Nature, 407*, 695-702, 2000.

Bray, S., T.W. Trull, and S. Manganini, *SAZ Project Moored Sediment Traps: Results of the 1997-1998 Deployments*, 128 pp, Antarct Coop. Res. Cent , Hobart, Tasmania, Australia, 2000.

Brewer, P.G., Nozaki, Y., Spencer, D.W. and Fleer, A.P., Sediment trap experiments in the Deep North Atlantic: Isotopic and elemental fluxes, *J. Mar. Res., 38*, 703-728, 1980.

Broecker, W.S. and T. Takahashi, The relationship between lysocline depth and in situ carbonate ion concentration, *Deep Sea Res., 25*. 65-95, 1978.

Bucciarelli, E., S. Blain, and P. Treguer, Iron and manganese in the wake of the Kerguelen islands (Southern Ocean), *Mar. Chem., 73*, 21-36, 2001.

Buesseler, K.O.. The decoupling of production and particulate export in the surface ocean, *Global Biogeochem. Cycles, 12*, 297-310, 1998.

Buma, A.G.J., P. Treguer, G.W. Kraay, and J. Morvan, Algal pigment patterns in different water masses of the Atlantic sector of the Southern Ocean during fall 1987, *Polar Biol., 11*, 55-62. 1990.

Caldeira, K., and P.B. Duffy, The role of the Southern Ocean in uptake and storage of anthropogenic carbon dioxide, *Science, 287*, 620-622, 2000.

Cardinal, D., F. Dehairs, T. Cattaldo, and L. André, Geochemistry of suspended particles in the Subantarctic and Polar Frontal Zones

south of Australia: Constraints on export and advection processes, *J. Geophys. Res.*, this issue.

Choi, M.S., R. Francois, K. Sims, M.P. Bacon, S. Brown-Leger, A.P. Fleer, L. Ball, D. Schneider, and S. Pichat, Rapid determination of ^{230}Th and ^{231}Pa in seawater by desolvated micro-nebulization inductively coupled plasma magnetic sector mass spectrometry. *Mar. Chem.*, in press, 2001.

Clementson, L.A., J.S. Parslow, F.B. Griffiths, V.D. Lyne, D.J. Mackey, G.P. Harris, D.C. McKenzie, P.I. Bonham, C.A. Rathbone, and S. Rintoul, Controls on phytoplankton production in the Australian sector of the subtropical convergence, *Deep Sea Res., Part I, 45*, 1627-1661, 1998.

Clementson, L.A., J.S. Parslow, A.R. Turnbull, D.C. McKenzie, and C.E. Rathbone, Optical properties of waters in the Australasian sector of the Southern Ocean, *J. Geophys. Res.*, this issue.

Collier, R., J. Dymond, S. Honjo, S. Manganini, R. Francois, and R. Dunbar, The vertical flux of biogenic and lithogenic material in the Ross Sea: Moored sediment trap observations 1996-1998, *Deep Sea Res., Part II, 47*, 3491-3520, 2000.

Comiso, J.C., C.R. McClain, C.W. Sullivan, J.P. Ryan, and C.L. Leonard, Coastal Zone Color Scanner pigment concentrations in the Southern Ocean and relationships to geophysical surface features, *J. Geophys. Res., 98*, 2419-2451, 1993.

Conte, M. and N. Ralph, Biological reprocessing of particle flux within meso and bathypelagic waters of the Sargasso Sea, *Eos Trans., AGU Ocean Sci. Meet. Suppl., 80* (49), 1999.

Cresswell, G.R., Currents of the continental shelf and upper slope of Tasmania, *R. Soc. Tasmania, 133*, 21-30, 2000.

Detmar, A.E. and U.V. Bathmann, Distribution patterns of autotrophic pico- and nanoplankton and their relative contribution to algal biomass during spring in the Atlantic sector of the Southern Ocean, *Deep Sea Res., Part II, 44*, 299-320, 1997.

Dunbar, R.B., A.R. Leventer, and D.A. Mucciarone, Water column sediment fluxes in the Ross Sea, Antarctica: Atmospheric and sea ice forcing, *J. Geophys. Res., 103*, 30,741-30,759, 1998.

England, M., The age of water and ventilation timescales in a global ocean model, *J. Phys. Oceanogr., 25*, 2756-2777. 1995.

Fischer, G., D. Futterer, R. Gersonde, S. Honjo, D. Ostermann, and G. Wefer, Seasonal variability of particle flux in the Weddel Sea and its relation to ice cover, *Nature, 335*, 426-428, 1988.

Fischer, G., V. Ratmeyer, and W. Wefer, Organic carbon fluxes in the Atlantic and the Southern Ocean: Relationship to primary production compiled from satellite radiometer data, *Deep Sea Res., Part II, 47*, 1961-1997, 2000.

Francois, R.F., M.A. Altabet, E.-F. Yu, D.M. Sigman, Bacon, M.P., M. Franck, G. Bohrman, G. Bareille, and L.D. Labeyrie, Water column stratification in the Southern Ocean contributed to the lowering of glacial atmospheric CO_2, *Nature*, 389, 929-935, 1997.

Frankignoulle, M., C. Canon, and J.-P. Gattuso, Marine calcification as a source of carbon dioxide: Positive feedback of increasing atmospheric CO_2, *Limnol. Oceanogr., 39*, 458-462, 1994.

Gille, S.T., Mean sea surface heigh' of the Antarctic Circumpolar Current from Geosat data: Method and application, *J. Geophys. Res., 99*, 18,255-18,273, 1994.

Griffiths, F.B., T.S. Bates, P.K. Quinn, L.A. Clementson, and J.S. Parslow, The oceanographic context of the first aerosol characterization experiment (ACE 1): A physical, chemical, and biological overview, *J. Geophys. Res., 104*, 21,649-21,671, 1999.

Holligan, P.M. and J.E. Robertson, Significance of ocean carbonate budgets for the global carbon cycle, *Global Change Biol., 2*, 85-95, 1996.

Honjo, S., Fluxes of particles to the interior of the open oceans, in *Particle Flux in the Ocean*, edited by V. Ittekkot et al., pp. 91-154, John Wiley, New York, 1996.

Honjo, S., The rain of ocean particles and Earth's carbon cycle, *Oceanus, 40*, 4-7, 1997.

Honjo, S. and S. Manganini, Biogenic particle fluxes at the 34°N 21°W and 48°N 21°W stations, 1989-1990: Methods and analytical data compilation, pp. 77, Woods Hole Oceanographic Institution, Woods Hole, Mass., 1992.

Honjo, S. and S.J. Manganini, Annual biogenic particle fluxes to the interior of the North Atlantic Ocean; studied at 34°N 21°W and 48°N 21°W stations, *Deep Sea Res., Part II, 40*, 587-607, 1993.

Honjo, S., R. Francois, S. Manganini, J. Dymond, and R. Collier, Particle fluxes to the interior of the Southern Ocean in the western Pacific sector along 170°W, *Deep Sea Res., Part II, 47*, 3521-3548, 2000.

Jacques, G., Is the concept of new production-regenerated production valid for the Southern Ocean, *Mar. Chem., 35*, 273-286, 1991.

Kalnay, E., et al., The NCEP/NCAR reanalysis project, *Bull. Am. Meterol. Soc., 77*, 437-471, 1996.

Keeling, C.D., T.P. Whorf, M. Wahlen, and J.V. Plicht, Interannual extremes in the rate of rise of atmospheric carbon dioxide since 1980, *Nature, 375*, 666-670, 1995.

Kopczynska, E.E., M. Fiala, and C. Jeandel, Annual and interannual variability in phytoplankton at a permanent station off Kerguelen Islands, Southern Ocean, *Polar Biol., 20*, 342-351, 1998.

Kopczynska, E.E., F. Dehairs, M. Elskens, and S. Wright, Phytoplankton and microzooplankton variability between the Subtropical and Polar Fronts south of Australia: Thriving under regenerative and new production in late summer, *J. Geophys. Res.* (this issue), 2001.

Kumar, N., R.F. Anderson, R.A. Mortlock, P.N. Froelich, P. Kubik, B. Dittrich-Hannen, and M. Suter, Increased biological productivity and export production in the glacial Southern Ocean, *Nature, 378*, 675-680, 1995.

Lampitt, R.S. and A.N. Antia, Particle flux in deep seas: Regional characteristics and temporal variability, *Deep Sea Res., Part I, 44*, 1377-1403, 1997.

Langone, L., M. Frignani, M. Ravaioli, and C. Bianchi, Particle fluxes and biogeochemical processes in an area influenced by seasonal retreat of the ice margin (northwestern Ross Sea, Antarctica), *J. Mar. Syst., 27*, 221-234, 2000.

Laubscher, R.K., R. Perissinotto, and C.D. McQuaid, Phytoplankton production and biomass at frontal zones in the Atlantic sector of the Southern Ocean, *Polar Biol., 13*, 471-481, 1993.

Laws, E.A., P.G. Falkowski, W.O.J. Smith, H. Ducklow, and J.J. McCarthy, Temperature effects on export production in the open ocean, *Global Biogeochem. Cycles, 14*, 1231-1246, 2001.

Lee, K., R. Wanninkhof, T. Takahashi, S.C. Doney, and R.A. Feely, Low interannual variability in recent oceanic uptake of atmospheric carbon dioxide, *Nature, 396*, 155-159, 1998.

Lefevre, N. and A.J. Watson, Modeling the geochemical cycle of iron in the oceans and its impact on atmospheric CO_2 concentrations, *Global Biogeochem. Cycles, 13*, 727-736, 1999.

Letelier, R.M., M.R. Abbot, and D.M. Karl, Chlorophyll natural fluorescence response to upwelling events in the Southern Ocean, *Geophys. Res. Lett., 24*, 409-412, 1997.

Lourey, M. and T.W. Trull, Seasonal nutrient depletion and carbon export in the Subantarctic and Polar Frontal Zones of the Southern Ocean south of Australia., *J. Geophys. Res.*, this issue.

Martin, J.H., G.A. Knauer, D.M. Karl, and W.W. Broenkow, VERTEX: Carbon cycling in the northeast Pacific, *Deep Sea Res., Part A, 34*, 267-285, 1987.

Martin, J.H., S.E. Fitzwater, and R.M. Gordon, Iron deficiency limits growth in Antarctic waters, *Global Biogeochem. Cycles, 4*, 5-12, 1990.

Matear, R. and A.C. Hirst, Climate change feedback on the future oceanic CO_2 uptake, *Tellus, 5*, 722-733, 1999.

Mcgillicuddy, D.J., A.R. Robinson, and J.J. Mccarthy, Coupled physical and biological modelling of the spring bloom in the north Atlantic (II): Three dimensional bloom and post-bloom processes, *Deep Sea Res., Part I, 42*, 1359-1398, 1995.

McNeil, B.I., B. Tilbrook, and R.J. Matear, Accumulation and uptake of anthropogenic CO_2 in the Southern Ocean south of Australia between 1968 and 1996, *J. Geophys. Res.*, this issue.

Mengesha, S., F. Dehairs, M. Fiala, M. Elskens, and L. Goeyens, Seasonal variation of phytoplankton community structure and nitrogen uptake regime in the Indian sector of the Southern Ocean, *Polar Biol., 20*, 259-272, 1998.

Metzl, N., B. Tilbrook, and A. Poisson, The annual fCO_2 cycle and the air-sea CO_2 flux in the sub-Antarctic Ocean, *Tellus Ser. B, 51*, 849-861, 1999.

Michaels, A.F. and M.W. Silver, Primary production, sinking fluxes and the microbial food web, *Deep Sea Res., Part A, 35*, 473-490, 1988.

Miquel, J.C., M. Carroll, and C. Jeandel, Seasonal trend in particulate carbon flux at the time-series site Kerfix in the Southern Ocean, *Ann. Geophys., 16*, Supp. II, 549, 1998.

Moore, J.K., M.R. Abbott, and J.G. Richman, Location and dynamics of the Antarctic Polar Front from satellite sea surface temperature data, *J. Geophys. Res., 104*, 3059-3073, 1999.

Morrow, R., R. Coleman, J. Church, and D. Chelton, Surface eddy momentum flux and velocity variances in the Southern Ocean from Geosat altimetry, *J. Phys. Oceanogr.*, *24*, 2050-2071, 1994.

Nodder, S.D. and L.C. Northcote, Episodic particulate fluxes at southern temperate mid-latitudes (42-45°S) in the Subtropical Front region, east of New Zealand, *Deep Sea Res., Part I*, *48*, 833-864, 2001.

Odate, T. and M. Fukuchi, Distribution and community structure of picophytoplankton in the Southern Ocean during the late austral summer of 1992, *Proc. NIPR Symp. Polar Biol.*, *8*, 86-100, 1995.

Olbers, D.J., V. Gouretski, and G.S.J. Schroter, *Hydrographic Atlas of the Southern Ocean*, 99 pp., Alfred Wegener Inst. for Polar and Mar. Res., Bremerhaven, Germany, 1992.

Orsi, A.H., T.I. Whitworth, and W.D.J. Nowlin, On the meridional extent and fronts of the Antarctic Circumpolar Current, *Deep Sea Res., Part I*, *42*, 641-673, 1995.

Parslow, J.S., P.W. Boyd, S.R. Rintoul, and F.B. Griffiths, A persistent subsurface chlorophyll maximum in the Interpolar Frontal Zone south of Australia: Seasonal progression and implications for phytoplankton-light-nutrient interactions, *J. Geophys. Res.*, this issue.

Phillips, H.E. and S.R. Rintoul, Eddy variability and energetics from direct current measurements in the Antarctic Circumpolar Current south of Australia, *J. Phys. Oceanogr.*, *30*, 3050-3076, 2000.

Pilskaln, C.H., C. Lehmann, J.B. Paduan, and M.W. Silver, Spatial and temporal dynamics in marine aggregate abundance, sinking rate, and flux: Monterey Bay, central California, *Deep Sea Res., Part II*, *45*, 1803-1837, 1998.

Popp, B.N., et al., Controls on the carbon isotopic composition of Southern Ocean phytoplankton, *Global Biogeochem. Cycles*, *13*, 827-843, 1999.

Pudsey, C J. and P. King, Particle fluxes, benthic processes and the palaeoenvironmental record in the northern Weddell Sea, *Deep Sea Res., Part I*, *44*, 1841-1876, 1997.

Rintoul, S.R., J.R. Donguy, and D H. Roemmich, Seasonal evolution of upper ocean thermal structure between Tasmania and Antarctica, *Deep Sea Res., Part I*, *44*, 1185-1202, 1997.Rintoul, S.R. and J.L. Bullister, A late winter hydrographic section from Tasmania to Antarctica, *Deep Sea Res., Part I*, *46*, 1417-1454, 1999.

Rintoul, S.R. and S. Sokolov, Baroclinic transport variability of the Antarctic Circumpolar Current south of Australia (WOCE repeat section SR3), *J. Geophys. Res.*, *106*, 2795-2814, 2001.

Rintoul, S.R. and T.W. Trull, Seasonal evolution of the mixed layer in the Subantarctic Zone south of Australia, *J Geophys. Res.*, this issue.

Rutgers van der Loeff, M.M., and G.W. Berger, Scavenging of ^{230}Th and ^{231}Pa near the Antarctic Polar Front in the South Atlantic, *Deep Sea Res., Part I*, *40*, 339-357, 1993.

Sarmiento, J.L. and M. Bender, Carbon biogeochemistry and climate change, *Photosyn. Res.*, *39*, 209-234, 1994.

Sarmiento, J.L. and C. LeQuere, Oceanic carbon dioxide uptake in a model of century-scale global warming, *Science*, *274*, 1346-1350, 1996.

Sarmiento, J.L., J.R. Toggweiler, and R. Najjar, Ocean carbon-cycle dynamics and atmospheric pCO_2 *Phil. Trans. R. Soc. London, Ser. A 325*, 3-21, 1988.

Shaffer, G., Effects of the marine carbon biota on global carbon cycling, in *The Global Carbon Cycle*, edited by M. Heimann, pp. 431-435, Springer-Verlag, New York, 1993.

Siegel, D. and W.G. Deuser, Trajectories of sinking particles in the Sargasso Sea: Modeling of statistical funnels above deep-ocean sediment traps, *Deep Sea Res., Part I*, *44*, 1519-1541, 1997.

Siegel, D.A., T.C. Granata, A.F. Michaels, and T.D. Dickey, Mesoscale eddy diffusion, particle sinking, and the interpretation of sediment trap data, *J. Geophys. Res.*, *95*, 5305-5311, 1990.

Sigman, D.M., M.A. Altabet, D.C. McCorkle, R. Francois, and G. Fischer, The δ^{15}N of nitrate in the Southern Ocean: Consumption of nitrate in surface waters, *Global Biogeochem. Cycles*, *13*, 1149-1166, 1999.

Smetacek, V., Role of sinking in diatom life-history cycles: Ecological, evolutionary and geological significance, *Mar. Biol.*, *84*, 239-251, 1985.

Smetacek, V., EisenEx: International team conducts iron experiment in Southern Ocean, *U.S. JGOFS News*, *11*, 11-14, 2001.

Smetacek, V., H.J.W. DeBaar, U.V. Bathmann, K. Lochte, and M.M. Rutgers van der Loeff, Ecology and biochemistry of the Antarctic Circumpolar Current during austral spring: a summary of Southern Ocean JGOFS cruise ANT X/6 of R.V. *Polarstern*, *Deep Sea Res., Part II*, *44*, 1-21, 1997.

Stephens, B.B. and R.K. Keeling, The influence of Antarctic sea ice on glacial-interglacial CO_2 variations, *Nature*. *404*, 171-174, 2000.

Taylor, S.R., Abundance of chemical elements in continental crust: A new table, *Geoch. Cosmochim. Acta*, *28*, 1273-1285, 1964.

Taylor, S.R. and S.M. McLennan, *The Continental Crust: Its Composition and Evolution*, 312 pp., Blackwell Sci., Malden, Mass., 1985.

van Leeuwe, M.A., H.J.W. de Baar, and M.J.W. Veldhuis, Pigment distribution in the Pacific region of the Southern Ocean (autumn 1995), *Polar Biol.*, *19*, 348-353, 1998.

von Bodungen, B., M. Wunsch, and H. Furderer, Sampling and analysis of suspended and sinking particles in the northern North Atlantic, in *Marine Particles: Analysis and Characterization*, *Geophys. Monogr. Ser.* vol. 63, edited by D.C. Hurd and D.W. Spencer, pp. 47-56, AGU, Washington, D.C., 1991.

Wang, X., R.J. Matear, and T.W. Trull, Modeling seasonal phosphate export and resupply in the Subantarctic and Polar Frontal Zones in the Australian sector of the Southern Ocean, *J. Geophys. Res.*, this issue.

Wefer, G. and G. Fischer, Annual primary production and export flux in the Southern Ocean from sediment trap data, *Mar. Chem.*, *35*, 597-613, 1991.

Wefer, G , G. Fischer, D. Fuetterer, and R. Gersonde, Seasonal particle flux in the Bransfield Strait, Antarctica, *Deep Sea Res., Part A*, *35*, 891-898, 1988.

Wong, C.S., F.A. Whitney, D.W. Crawford, K. Iseki, R.J. Matear W.K. Johnson, J S. Page, and D. Timothy, Seasonal and interannual variability in particle fluxes of carbon, nitrogen and silicon from time series of sediment traps at Ocean Station P, 1982-1993: relationship to changes in subarctic primary productivity, *Deep Sea Res , Part II*, *46*, 2735-2760, 1999.

Wright, S.W., D.P. Thomas, H.J. Marchant, H.W. Higgins, M.D Mackey, and D.J. Mackey, Analysis of phytoplankton of the Australian sector of the Southern Ocean: Comparisons of microscopy and size frequency data with interpretations of pigment HPLC data using the 'CHEMTAX' matrix factorisation program, *Marine Ecol Prog. Ser.*, *144*, 285-298, 1996.

Yu, E.-F., R. Francois, M.P. Bacon, S. Honjo, A.P. Fleer, S.J. Manganini, M.M. Rutgers van der Loeff, and V Ittekot, Trapping efficiency of bottom-tethered sediment traps estimated from the intercepted fluxes of ^{230}Th and ^{231}Pa, *Deep Sea Res., Part I*, *48*, 865-889, 2001.

S. G. Bray and T. W. Trull, Antarctic CRC, GPO Box 252-80, Hobart Tasmania 7001, Australia. (Tom.Trull@utas.edu.au)

S. Honjo, R. François, and S. J. Manganini, Woods Hole Oceanographic Institution, Woods Hole, MA 02543, USA.

(Received March 15, 2000; revised May 18, 2001; accepted May 24, 2001.)